

This author's accepted manuscript may be used for non-commercial purposes in accordance with [Wiley Terms and Conditions for Self-Archiving](#).

The full details of the published version of the article are as follows:

TITLE: The role of chick Ebf genes in the mediolateral patterning of the somites

AUTHORS: Mohammed A. El-Magd, Shafika A. Elsayed, Eman S. El-Shetry, Ahmed Abdelfattah-Hassan, Ayman A. Saleh, Steve Allen, Imelda McGonnell, Ketan Patel

JOURNAL: genesis: The Journal of Genetics and Development

PUBLISHER: Wiley

PUBLICATION DATE: 13 November 2019

DOI: <https://doi.org/10.1002/dvg.23339>

# The role of chick Ebf genes in the mediolateral patterning of the somites

Mohammed A. El-Magd<sup>\*1</sup>, Shafika A. Elsayed<sup>2</sup>, Eman S. El-Shetry<sup>3</sup>, Ahmed Abdelfattah-Hassan<sup>4</sup>,  
Ayman A. Saleh<sup>5</sup>, Steve Allen<sup>6</sup>, Imelda McGonnell<sup>6</sup>, Ketan Patel<sup>7</sup>

<sup>1</sup> Department of Anatomy and Embryology, Faculty of Veterinary Medicine, Kafrelsheikh University, Egypt

<sup>2</sup> Department of Histology and Cytology, Faculty of Veterinary Medicine, Zagazig University, Egypt

<sup>3</sup> Department of Human Anatomy and Embryology, Faculty of Medicine, Zagazig University, Egypt

<sup>4</sup> Department of Anatomy and Embryology, Faculty of Veterinary Medicine, Zagazig University, Egypt

<sup>5</sup> Department of Animal Wealth Development, Genetics and Genetic Engineering, Faculty of Veterinary Medicine, Zagazig University, Egypt

<sup>6</sup> Department of Veterinary Basic Sciences, Royal Veterinary College, London, United Kingdom

<sup>7</sup> School of Biological Sciences, University of Reading, Reading, United Kingdom

Mohammed A. El-Magd, Department of Anatomy and Embryology, Faculty of Veterinary Medicine, Kafrelsheikh University, Egypt.

Email: [mohamed.abouelmagd@vet.kfs.edu.eg](mailto:mohamed.abouelmagd@vet.kfs.edu.eg)

## Summary

This study was conducted to check whether the three chick Early B-cell Factor (*Ebf*) genes, particularly *cEbf1*, would be targets for Shh and Bmp signals during somites mediolateral (ML) patterning. Tissue manipulations and gain and loss of function experiments for Shh and Bmp4 were performed and the results revealed that *cEbf1* expression was initiated in the cranial presomitic mesoderm by low dose of Bmp4 from the lateral mesoderm and maintained in the ventromedial part of the epithelial somite and the medial sclerotome by Shh from the notochord; while *cEbf2/3* expression was induced and maintained by Bmp4 and inhibited by high dose of Shh. To determine whether *Ebf1* plays a role in somite patterning, transfection of a dominant-negative construct was carried out; this showed suppression of *cPax1* expression in the medial sclerotome and upregulation and medial expansion of *cEbf3* and *cPax3* expression in sclerotome and dermomyotome, respectively, suggesting that *Ebf1* is important for ML patterning. Thus, it is possible that low doses of Bmp4 set up *Ebf1* expression which, together with Shh from the notochord, leads to establishment of the medial sclerotome and suppression of lateral identities. These data also conclude that Bmp4 is required in both the medial and lateral domain of the somitic mesoderm to keep the ML identity of the sclerotome through maintenance of *cEbf* gene expression. These striking findings are novel and give a new insight on the role of Bmp4 on mediolateral patterning of somites

---

## 1 INTRODUCTION

The chick *Ebf* (early B-cell factor) genes are members of a novel highly conserved family of atypical helix–loop–helix (HLH) transcription factors, EBF. The chick embryo has three EBF proteins encoded by distinct genes, designated *cEbf1* through *3* (El-Magd, Allen, McGonnell, Otto, & Patel, 2013; Mella, Soula, Morello, Crozatier, & Vincent, 2004). EBF proteins are composed of five domains; DNA binding domain (DBD), immunoglobulin-like plexins transcription factor (IPT), atypical HLH, transactivation I domain (TSI), and transactivation II (TSII) domain and are originally discovered in rodents as a protein that regulates the

differentiation of B-lymphocyte (Crozatier, Valle, Dubois, Ibsouda, & Vincent, 1996). Our previous studies in addition to others demonstrated the importance of EBF for tissue specification, differentiation, and cell movements during development of nervous, adipose, muscular, and skeletal tissues as well as feathers and bone marrow (El-Magd, Saleh, El-Aziz, & Salama, 2014; El-Magd, Sayed-Ahmed, Awad, & Shukry, 2014; Moruzzo et al., 2017; Seike, Omatsu, Watanabe, Kondoh, & Nagasawa, 2018; Tolkin & Christiaen, 2016; Zee et al., 2013).

The mesoderm is subdivided along the mediolateral (ML) direction into somites and the lateral (intermediate and lateral plate) mesoderm, with a sharp morphological boundary between them (Danesh, Villasenor, Chong, Soukup, & Cleaver, 2009; Schoenwolf, Garcia-Martinez, & Dias, 1992). The medial and lateral parts of somites are derived from cells in different parts of the primitive streak/node (Psychoyos & Stern, 1996; Selleck & Stern, 1991). This ML subdivision corresponds functionally to the segregation between epaxial and hypaxial musculature and is independent of dermomyotome/sclerotome subdivision (Ordahl & Le Douarin, 1992; Pourquie et al., 1996; Pourquie, Coltey, Breant, & Le Douarin, 1995). Some genes are differentially expressed along the ML axis of the somites, such as *SWiP1* (expressed in the medial part of somite), *Pax1*, and *Ebf1* (expressed mainly in the medial sclerotome), *Ebf3* (expressed in the lateral sclerotome), *Pax3* (expressed throughout the dermomyotome, with elevated levels only in the lateral dermomyotomal lips), and *Sim1* (labeled first the entire lateral half of the epithelial somite, and then the lateral dermomyotome and sclerotome; (El-Magd et al., 2013; El-Magd et al., 2015; Olivera-Martinez, Missier, Fraboulet, Thélou, & Dhouailly, 2002; Pourquie et al., 1996; Stern & Piatkowska, 2015; Tonegawa et al., 1997; Vasiliauskas, Hancock, & Stern, 1999).

Different levels of Bmp4 activity control the ML subdivision of the mesoderm: a high level produces the lateral plate, whereas a moderate level forms the intermediate mesoderm and a low level determines the lateral portion of the somite (Pourquie et al., 1996; Tonegawa et al., 1997). Although the notochord expresses both Chordin and Noggin as inhibitors of BMP, only Noggin can antagonize the lateralization effect of the lateral mesoderm-derived Bmp4 on the paraxial mesoderm (McMahon et al., 1998; Stafford, Brunet, Khokha, Economides, & Harland, 2011; Stafford, Monica, & Harland, 2014; Streit & Stern, 1999). Any disturbance in the balance between the lateralizing and medializing effects of Bmp4 and Noggin, respectively, results in a loss of ML polarity of the paraxial and lateral plate mesoderm (reviewed by Stern & Piatkowska, 2015). In line with this idea, when the presumptive part of the crPSM forming somite is transplanted into the lateral plate-fated region of chick embryo, the somite is respecified to lateral plate mesoderm (Garcia-Martinez & Schoenwolf, 1992) due to the lateralizing effect of Bmp4 (Pourquie et al., 1996; Tonegawa et al., 1997). Conversely, the lateral plate-fated tissue is redirected to the somite when transplanted into the paraxial mesoderm region (Garcia-Martinez & Schoenwolf, 1992), and this effect is attributed to the notochord-derived Noggin (Pourquie et al., 1996; Tonegawa et al., 1997). In addition, implantation of Bmp4 expressing cells between the neural tube (NT) and PSM induces expression of the lateral dermomyotomal/sclerotomal marker *Sim1* in the medial regions of the dermomyotome/sclerotome of the differentiated somites, resulting in lateralization of the somites (Pourquie et al., 1996). Moreover, somites of embryos with higher Bmp signaling are smaller and lost caudally because paraxial mesoderm cells are aberrantly specified as lateral mesoderm (Stafford et al., 2014). Likewise, loss of BMP4 relieves the lateralization of the paraxial mesoderm observed in Noggin mutant embryos (Wijgerde, Karp, McMahon, & McMahon, 2005). Similarly, ectopic application of Noggin expressing cells in the presumptive lateral plate mesoderm results in ectopic somites (Tonegawa & Takahashi, 1998). In addition to Noggin, Shh is also required to maintain the medial identity of the somites through regulation of the medial sclerotomal marker, *Pax1* (Borycki, Mendham, & Emerson, 1998; Cairns, Sato, Lee, Lassar, & Zeng, 2008).

The medial somitic marker *SWiP-1* and the lateral somitic marker *Sim1* are regulated by *Shh* (from the notochord) and *Bmp4* (from lateral plate/dorsal ectoderm), respectively (Pourquie et al., 1996; Vasiliauskas et al., 1999). These previous two studies showed clearly that despite the different cellular origins of medial and lateral somite cells, it is possible to alter the medial or lateral properties within a somite by signals from adjacent tissues. Our previous studies also showed that *cEbf1* expression in the medial sclerotome is regulated by *Shh* signals from the notochord/floor plate and *cEbf2,3* expression in the lateral sclerotome is regulated by lateral mesoderm-derived *Bmp4* signals (El-Magd et al., 2013, 2015). Although, these earlier data on *cEbf* gene regulation in the somite are consistent with the known roles of Shh and Bmp in the mediolateral patterning

of somites, they do not address the effect of either the axial structures (notochord/floor plate) and different concentrations of Shh on *cEbf2/3* or the lateral plate mesoderm and Bmp4 on *cEbf1* expression in somites. Moreover, regulation of early *cEbf1* expression in the crPSM was not addressed in our previous studies. Therefore, we conducted this study to fill in these gaps and to check whether *cEbf*s, particularly *cEbf1*, could be downstream targets in *Shh* and *Bmp4* signaling cascade regulating the mediolateral patterning of the somites. To reach this goal, we constructed a negative dominant form of Ebf1 to monitor mediolateral patterning of somites through investigation of changes in medial and lateral somitic markers.

## 2 RESULTS

### 2.1 Tissues control *cEbf*s gene expression along the mediolateral axis of somitic mesoderm

In our previous studies, we have performed the following three tissue manipulation experiments to determine tissues regulating *cEbf* genes in somites: notochord ablation for *cEbf1*, lateral barrier insertion, and NT ablation for *cEbf2/3* (El-Magd et al., 2013, 2015). However, these three manipulations are not enough to get a final conclusion about the mediolateral regulation of these genes. Therefore, in the present study, we performed some additional tissue manipulation experiments, including medial barrier insertion, removal of axial structures, notochord ablation (for *cEbf2/3*), and NT ablation and lateral barrier insertion (for *cEbf1*), to detect the effect of the axial structures on the lateral sclerotomal markers, *cEbf2/3*, and the effect of the lateral mesoderm and NT on the medial sclerotomal marker, *cEbf1*.

Table 1 shows all details regarding the tissue manipulations including the manipulation stages (at operation time and at the end of reincubation), manipulation site (either crPSM or epithelial somites), and number of embryos showing the phenotype and altered *cEbf* genes expression.

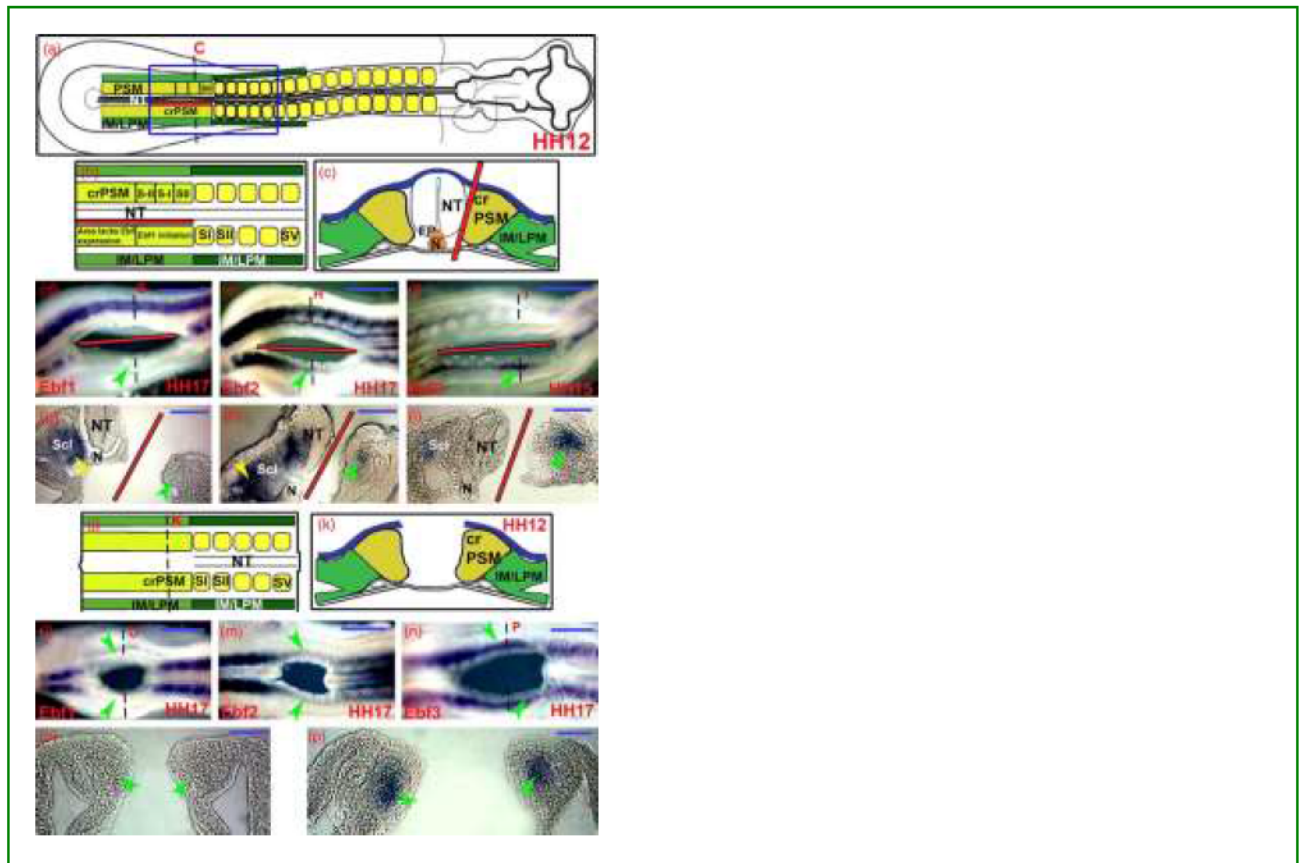
**Table 1** Details of the tissue manipulation experiments

Name of manipulation	Anatomical region	Stage manipulation was performed	Stage embryos were harvested	Number of embryos alive at harvesting	Number of embryos showing a phenotype or an altered gene expression		
					<i>cEbf1</i>	<i>cEbf2</i>	<i>cEbf3</i>
Medial barrier insertion	crPSM	HH11-HH12	HH15-HH17	21	7	6	6
Axial structures ablation	crPSM	HH12	HH17	21	7	6	6
Medial barrier insertion	ES	HH12	HH17	21	7	6	6
Medial barrier insertion	caPSM	HH14	HH17	5	5	–	–
Notochord removal	crPSM	HH12	HH16-HH17	20	–	8	8
Neural tube ablation	crPSM	HH12	HH16	12	12	–	–
	ES	HH12	HH17	10	10	–	–
Lateral barrier insertion	crPSM	HH12	HH17	7	6	–	–
	ES	HH12	HH17	7	6	–	–
New culture (control)	WE	HH12	HH17	14	–	7	7
Cyclopamine treatment	WE	HH12	HH17	14	–	6	6
Control PBS beads	crPSM	HH12-HH13	HH17-HH18	8	–	2	6
SHH beads (0.5 µg/µl)	crPSM	HH12-HH13	HH17-HH18	20	–	10	10
SHH beads (1 µg/µl)	crPSM	HH12-HH13	HH17-HH18	20	–	8	9
SHH beads (2 µg/µl)	crPSM	HH12-HH13	HH17-HH18	20	–	8	8
DF-1 cells (control)	Lateral to crPSM	HH12	HH18	7	6	–	–
Noggin secreting cells	Lateral to crPSM	HH12	HH18	7	6	–	–
Noggin secreting cells	Lateral to ES	HH12	HH18	7	6	–	–
DF-1 cells (control)	Lateral to ES	HH12	HH17-HH18	7	6	–	–
Noggin secreting cells	Medial to crPSM	HH12	HH17-HH18	7	6	–	–
Noggin secreting cells	Medial to ES	HH12	HH17-HH18	7	7	–	–
Bmp4 beads (50 µg/ml)	crPSM	HH11-HH13	HH17-HH18	8	7	–	–
Bmp4 beads (100 µg/ml)	crPSM	HH12	HH17	7	7	–	–
Bmp4 beads (150 µg/ml)	crPSM	HH12	HH17	7	7	–	–

Abbreviations: caPSM, caudal part of presomitic mesoderm; crPSM, cranial part of presomitic mesoderm; ES, epithelial somites; WE, whole embryo.

### 2.1.1 Effect of medial barrier insertion and removal of axial structures on *cEbf* gene expression

To investigate the influence of signals from axial structures on *cEbf* gene expression, both the notochord and the NT were separated from the crPSM by an aluminum foil barrier spanning 5–8 prospective somites of chick embryos (Figure 1a–c). This manipulation resulted in very small somites (Marcelle, Ahlgren, & Bronner-Fraser, 1999; Teillet et al., 1998), which showed complete down-regulation of *cEbf1* expression in the sclerotome at the operation side as compared to the control nonoperated side (green vs. yellow arrowheads, Figure 1d,g), slight down-regulation of *cEbf2* sclerotomal expression in the cranial operation region (arrowheads, Figure 1e,h), and up-regulation of *cEbf3* expression in the lateral sclerotomal portion with slight medial expansion (arrowheads, Figure 1f,i).



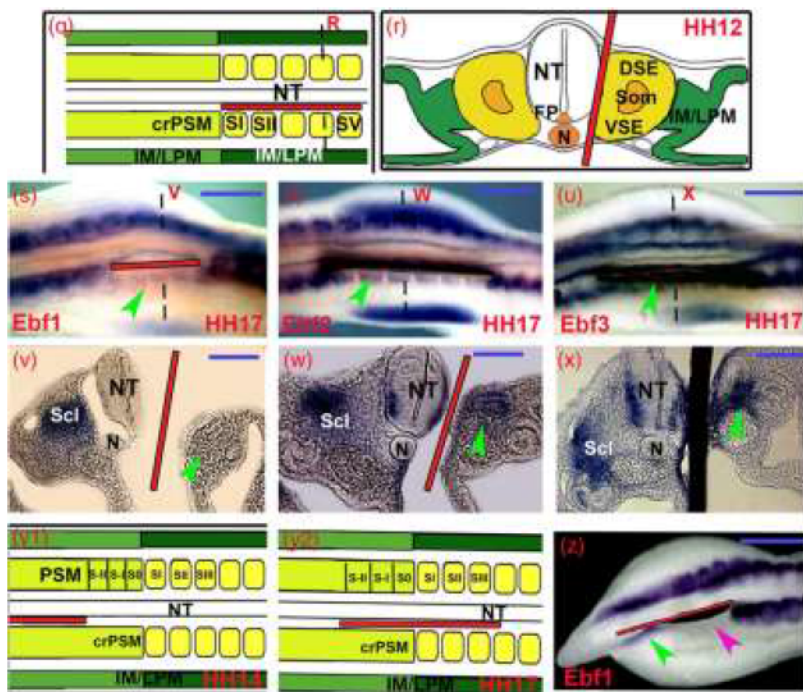


**Figure 1** Effect of medial barrier insertion and axial structures removal on *cEbf* gene expression. (a) Schematic diagram of HH12 chick embryo before commencement of the microsurgery showing the operation sites (boxed region). All whole mount panels are oriented in a similar way to this embryo. (b, c) Schematic diagrams (b, dorsal view) and (c, transverse section) showing the position of a medial barrier (red line) inserted between the axial structures (the NT and notochord) and the crPSM. (d–i) Whole mount in situ hybridization and transverse sections following barrier insertion between the axial structures and crPSM. (j, k) Schematic diagrams showing the operation site of axial structures ablation at level of crPSM. (l–p) HH17 chick embryos after ablation of axial structures at crPSM level. (q, r) Schematic diagrams showing the position of a medial barrier (red line) inserted between the axial structures and the newly formed five somites (from SI to SV). (s–x) HH17 chick embryos after medial barrier insertion between axial structures and epithelial somites. (y) Schematic diagrams showing the position of a medial barrier (red line) between the axial structures and the caudal portion of the PSM (Y1) and the position of this barrier after 8–10 hr incubation (Y2). (z) HH17 chick embryos after medial barrier insertion at level shown in Y2. In all photos, dashed lines indicate the site of transverse sections. Abbreviations: crPSM, cranial presomitic mesoderm; DSE, dorsal somitic epithelia; FP, floor plate; IM, intermediate mesoderm; LPM, lateral plate mesoderm; N, notochord; NT, neural tube; PSM, presomitic mesoderm; (SI–SV), somites 1–5; Scl, sclerotome; Som, somitocoele; VSE, ventral somitic epithelia. Scale bars: d–f, l–n, s–u, z = 400  $\mu$ m, g–i, o, p, v–x = 150  $\mu$ m

To confirm these medial barrier results, the axial structures were ablated at the crPSM level (Figure 1j,k). These manipulations gave the same results as using medial barrier at the same level; lack of *cEbf1* expression in the ill-developed somites on both sides of the ablated region (arrowheads, Figure 1l,o), slight reduction of *cEbf2* expression (arrowheads, Figure 1m) and an increase of *cEbf3* expression (arrowheads, Figure 1n,p).

To check the effect of axial tissues on the maintenance of *cEbf* genes expression, the medial barriers were inserted between the epithelial somites (from SI to SV) and the axial structures (Figure 1q,r). The obtained results revealed the presence of small somites and complete loss of *cEbf1* expression (arrowheads, Figure 1s,v), slight down-regulation of *cEbf2* expression (arrowheads, Figure 1t,w) and disorganized, but retained expression of *cEbf3* (arrowheads, Figure 1u,x) in the sclerotome lateral to the barrier.



Tissues regulation of the early *cEbf1* expression in the crPSM was not investigated in our previous studies (El-Magd et al., 2013, 2015). Given that isolation of the PSM from the axial structures causes a striking reduction in somite size due to increased apoptosis (Dietrich, Schubert, & Lumsden, 1997), it is possible that the absence of *cEbf1* following ablation of the notochord (El-Magd et al., 2015) may be secondary to failure of *cEbf1*-expressing cells to develop and hence the notochord and probably Shh may not be the initial inducer of *cEbf1* expression. To check whether the axial structures can induce *cEbf1* expression in the crPSM, medial barriers were inserted at the level of the caudal PSM in a region spanning six prospective somites (Figure 1Y1,Y2). The embryos were operated at HH14 and reincubated for short time (~8–10 hr, HH17). During HH14 stage, only *cEbf1* expression has already initiated in the cranial portion of the crPSM in a region of three prospective somites length (from So to S-II) as previously described (El-Magd et al., 2015). During this 8–10 hr incubation period, the crPSM lateral to the barrier was deprived of contact with the axial structures. The PSM lateral to the barrier was formed properly and expressed *cEbf1* at a slightly reduced level compared to the nonoperated side (green arrowhead, Figure 1z). As expected, no *cEbf1* expression in somites formed next to the cranial region of the barrier (magenta arrowhead, Figure 1z). This indicates that the axial structures are mainly required for maintenance, rather than induction, of *cEbf1* expression.

In general, these experiments reveal that the NT and/or notochord are (is) important for maintenance of *cEbf1* expression and to a lesser extent for induction and maintenance of *cEbf2* expression in the somite. In contrast, these axial structures appear to repress *cEbf3* expression.

### 2.1.2 Effect of notochord removal on *cEbf2* and *cEbf3* gene expression

Our previous notochord ablation experiment revealed that *cEbf1* expression in the medial sclerotome is regulated by notochord signals (El-Magd et al., 2015). In contrast, *cEbf2* and *cEbf3* are expressed laterally in the sclerotome (El-Magd et al., 2013) and so they may be inhibited by medial signals from the notochord. To check this, the notochord-floor plate complex was removed at the crPSM level, a length of 4–6 prospective somites (Figure 2a). This operation prevents the development of ventral identities in the somite (Dietrich et al., 1997) resulting in delayed maturation of somites up to SVII (normally maturation occurs at SIV-V). These somites become smaller and have sharp boundaries. This operation led to loss of *cEbf2* expression in the ventromedial epithelial somites and became localized only in the somitocoele (green arrowheads, Figure 2c,e). However, this manipulation increased *cEbf3* expression in the medial somitic domain (green arrowheads, Figure 2d,f) as compared to the control (non-operated) embryo (green arrowhead, Figure 2b). These findings suggest that the notochord may partially regulate the medial expression of *cEbf2* in the immature somites. However, it may produce signal(s) that antagonize the lateral expression of *cEbf3*.

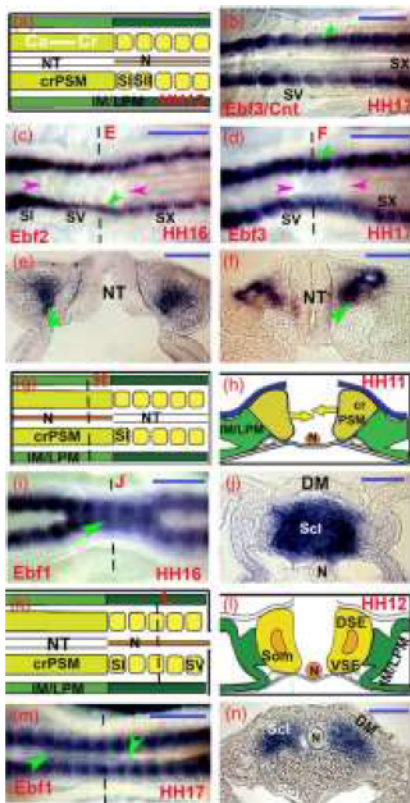


**Figure 2** The effect of notochord removal, and neural tube (NT) removal on *cEbf*s expression. (a) Schematic diagrams showing the operation site of axial notochord ablation at level of crPSM. (b) Whole mount in situ hybridization shows *cEbf3* expression in control (nonoperated) embryo. (c–f) Whole mount in situ hybridization and transverse sections at the levels of SVI following notochord and floor plate removal at crPSM level. (g, h) Schematic diagrams showing the operation site of NT ablation at level of crPSM. (i, j) Chick embryos following NT removal at crPSM show *cEbf1* expression. (k, l) Schematic diagrams showing the operation site of NT ablation at level of epithelial somites. (m, n) Chick embryos following NT removal at epithelial somites. The regions between the two magenta and the two green arrowheads are the operation sites. In all photos, dashed lines indicate the site of transverse sections. Abbreviations: crPSM, cranial presomitic mesoderm; DSE, dorsal somitic epithelia; FP, floor plate; IM, intermediate mesoderm; LPM, lateral plate mesoderm; N, notochord; NT, neural tube; PSM, presomitic mesoderm; SI–SV, somites 1–5; Scl, sclerotome; Som, somitocoele; VSE, ventral somitic epithelia. Scale bars: b–d, i, m = 400  $\mu$ m, e, f, j, l = 150  $\mu$ m

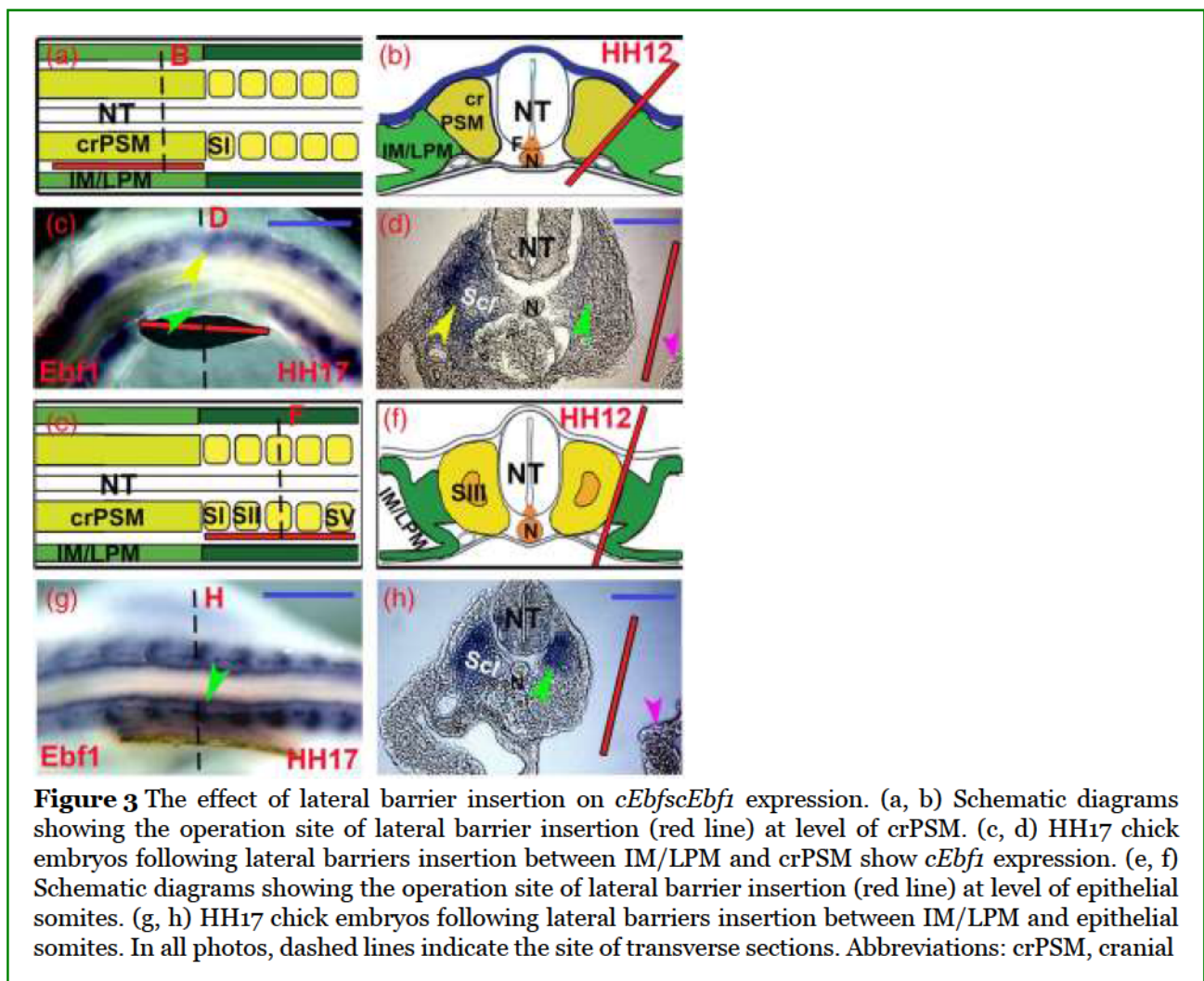
### 2.1.3 Neural tube ablation does not affect *cEbf* expression

Our previous study showed that NT ablation does not change *cEbf2,3* expression in the somites (El-Magd et al., 2013). Although, we know from our previous study that *cEbf1* regulation is mediated by signals from the notochord (El-Magd et al., 2015), it is also important to check whether the NT plays a role in that regulation. To determine this effect, the NT alone was removed at the level of the crPSM of HH11 embryos (Figure 2g,h). This operation often leads to the pairwise fusion of right and left crPSM forming a singular row of somites comprising of a dorsal epithelia cap (thought to be dermomyotome) and a ventral mesenchymal tissue (the sclerotome) (arrowhead, Figure 2i,j). Despite the absence of the NT and the new midline location of the somites, *cEbf1* gene expression remained relatively unchanged in the entire sclerotome ventral to the fused dorsal dermomyotome and adjacent to the notochord. The NT is therefore not necessary for induction of *cEbf1* expression in epithelial somites.

To check whether the NT can maintain *cEbf1* gene expression in somites, the NT was ablated at the level of the newly formed five somites of HH12 embryos (Figure 2k,l). After ~16 hr of reincubation, normal *cEbf1* expression was remained in the sclerotomal cells around the notochord (Figure 2m,n). Thus, the NT has no role in maintenance of *cEbf1* expression in somites.

#### 2.1.4 Effect of lateral structures on *cEbf1* gene expression in the somites

We have previously found that *cEbf2* and *cEbf3* expression in the lateral sclerotome is regulated by *Bmp4* signals from the lateral mesoderm (intermediate [IM] and lateral plate mesoderm [LPM]; El-Magd et al., 2013). In addition, results of the current study reported that the initiation of *cEbf1* expression in the crPSM in isolation from axial structures also argues for induction of *cEbf1* by other surrounding structures. Taken together, it is therefore possible that the lateral structures can initiate the *cEbf1* expression in somites. To test this possibility, the crPSM of HH12 embryo was separated from the IM/LPM by insertion of an impermeable barrier with length of 5–9 prospective somites (Figure 3a,b). Surprisingly, *cEbf1* expression was completely lost in the sclerotome medial to the barrier unlike the control somites on the contralateral sides (green arrowhead, Figure 3c,d). Insertion of barriers between the newly formed 5–8 somites and the IM/LPM (Figure 3e,f) resulted in a slight reduction in the most lateral edge of the *cEbf1* expression domain in the sclerotome (arrowhead, Figure 2g,h). These findings indicate that the lateral tissues or factors emanating from them are essential for induction, but not for maintenance, of the *cEbf1* expression in the somites.



presomitic mesoderm; FP, floor plate; IM, intermediate mesoderm; LPM, lateral plate mesoderm; N, notochord; NT, neural tube; SI-SV, somites 1–5; Scl, sclerotome. Scale bars: c, g = 400  $\mu\text{m}$ , d, h = 150  $\mu\text{m}$

## 2.2 Molecular regulation of *Ebfs* gene expression

Our previous studies showed that Shh mediates the signal from the notochord that maintains *cEbf1* gene expression in somites (El-Magd et al., 2015) and that the lateral plate-derived Bmp4 induces and maintains *cEbf2* and *cEbf3* expression in somites (El-Magd et al., 2013). In these two previous studies, the effect of Shh on *cEbf2/3* and the effect of Bmp4 on *cEbf1* were not addressed. Again to get an overall view regarding the mediolateral regulation of *cEbf* genes in the somites, herein we used Shh and Bmp4 gain and loss of function experiments to determine this effect.

### 2.2.1 Effect of inhibition of Shh by cyclopamine on *cEbf2* and *cEbf3* expression

To identify whether *cEbf2* and *cEbf3* expression could be altered upon specific inhibition of Shh, embryos were placed in a New culture system and treated with cyclopamine as was previously described (El-Magd et al., 2015). Loss of *cPax1* expression in cyclopamine-treated embryos as compared to control (untreated) embryos, confirmed that *Shh* has been successfully inhibited by this treatment (Figure 4a,b). Morphological characteristics were also used to ascertain that Shh was successfully inhibited. Some head malformations, including holoprosencephaly (blue arrowhead, Figure 4e), ill-developed mesencephalon (yellow arrowhead, Figure 4e), and atrophied pharyngeal arches especially the first arch (black arrowhead, Figure 4e), were occurred 1 day after cyclopamine treatment similar to cyclopamine-induced malformations reported by our previous study and by other studies (Cordero et al., 2004; El-Magd et al., 2015; Incardona, Gaffield, Kapur, & Roelink, 1998). Although, there was no cyclopia, as embryos were treated after formation of optic vesicle, the two eyes developed closer to each other (magenta arrowhead, Figure 4e). In contrast, the same stage control embryos did not show such malformations (Figure 4f). Unlike complete loss of *cEbf1* in cyclopamine-treated embryos (El-Magd et al., 2015), the expression of *cEbf2* (Figure 4c) and *cEbf3* (Figure 4e) in cyclopamine-treated embryos was similar to that in the control embryos (Figure 4d,f). Therefore, *Shh* is not the notochordal signaling molecule that either induces *cEbf2* or inhibits *cEbf3* somitic expression.



**Figure 4** Effect of Shh gain and loss function on *cEbf2* and *cEbf3* expression. (a–f) Whole mount in situ hybridization of HH16–HH17 embryos following either cyclopamine (a, c, e) or PBS (control; b, d, f) treatment shows expression of *cPax1*, *cEbf2*, and *cEbf3*. (g, h) Schematic diagrams, (g, dorsal view) and (h, transverse section) show the position of the implanted Affigel bead (arrowheads). (i–v) HH17–18 embryos following implantation of either PBS beads (i, j), or SHH beads at concentrations of 0.5  $\mu\text{g}/\mu\text{l}$  (k–n), 1  $\mu\text{g}/\mu\text{l}$  (o–r), and 2  $\mu\text{g}/\mu\text{l}$  (s–v) in the crPSM. The magenta arrowheads refer to the beads. Abbreviations: Ca, caudal; Cr, cranial; crPSM, cranial presomitic mesoderm; IM, intermediate mesoderm; LPM, lateral plate mesoderm; N, notochord; NT, neural tube; PBS, phosphate buffered saline; PSM, presomitic mesoderm; SI–SV, somites 1–5. Scale bars: a–f = 1 mm, i = 300  $\mu\text{m}$ , k, m, o, q, s, u = 350  $\mu\text{m}$ , j, l, n, p, r, t, v = 150  $\mu\text{m}$

### 2.2.2 Ectopic expression of Shh down-regulates *cEbf2* and *cEbf3* somitic expression

To check the effect of Shh ectopic expression on *cEbf2* and *cEbf3* expression in somites, phosphate buffered saline (PBS; as control) or Shh-loaded Affigel beads were implanted into the crPSM (magenta arrowheads, Figure 4). The control embryos, implanted with PBS beads (magenta arrowheads) showed normal *cEbf3* expression in the sclerotome and there is a normal developed dermomyotome (Figure 4gi,hj). However, implantation of 0.5  $\mu\text{g}/\mu\text{l}$  Shh-loaded beads (magenta arrowheads) resulted in either unaffected, or very slightly reduced somitic expression of *cEbf2* and *cEbf3* (Figure 4).

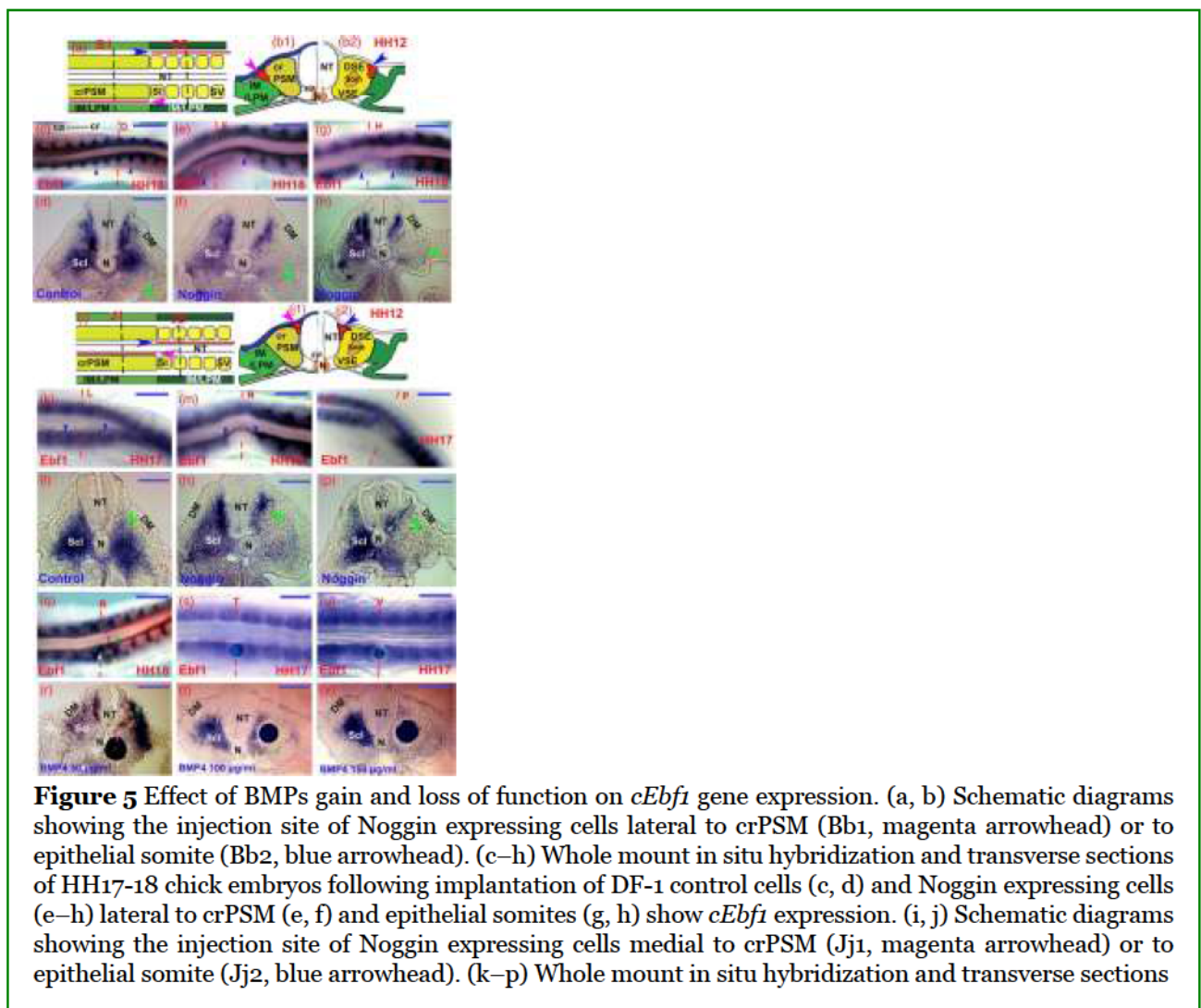
Because *Shh* acts as a morphogen, that is, it has a dose-dependent function, we tested whether higher concentration of Shh can alter the expression of *cEbf2* and *cEbf3* genes. Loading beads (magenta arrowheads) with 1  $\mu\text{g}/\mu\text{l}$  Shh slightly decreased the intensity, but not the domain, of *cEbf2* and *cEbf3* expression (Figure 4m,po-r). Moreover, much higher concentration 2  $\mu\text{g}/\mu\text{l}$  completely down regulates the expression of *cEbf2* and *cEbf3* in the somites (Figure 4).

These results indicated that only a very high dose of exogenous Shh can antagonize the lateral signals which are necessary to keep the lateral identity of *cEbf2* and *cEbf3* expressing cells. However, in the absence of any

information on the concentration of Shh protein that diffuses out of the bead, estimation of the effective dose of Shh remains speculative.

### 2.2.3 Inhibition of Bmp2/4 blocks *cEbf1* gene expression

Experimentally, Bmp2/4 function can be abrogated by local implantation of chick DF-1 fibroblast cells transfected with a mammalian *Noggin*-RCASBP(A) virus (El-Magd et al., 2013). In this prior study, we found that implantation of Noggin secreting cells medial to the crPSM resulted in a complete loss of *cEbf2* and a partial loss for *cEbf3* expression (El-Magd et al., 2013). However, when these cells were implanted medial to the epithelial somites, they resulted in a slight loss of *cEbf2* and *cEbf3* expression. Because barrier insertion experiments indicate the necessity for lateral signal(s) in initiation of *cEbf1* gene expression in somites, herein, we used the same experiment to evaluate whether endogenous *Bmp2/4*, which expressed abundantly in the lateral mesoderm and is crucial for mediolateral patterning of somites, can regulate expression of *cEbf1* gene. To check this possibility, pellets of chick DF-1 fibroblast cells transfected with a mammalian *Noggin*-RCASBP(A) virus or with empty vector (control) were implanted lateral or medial to crPSM or epithelial somites (arrowheads, Figure 5a,Bb1,Bb2,Ii,Jj1,Gj2). Injection of Noggin secreting cells lateral to the crPSM (arrowheads, Figure 5e,f) or epithelial somites (arrowheads, Figure 5g,h) resulted in complete loss of *cEbf1* expression in the sclerotome as compared to opposite somites and to control embryos (Figure 5c,d). These findings indicate that Bmp signals are necessary for induction and maintenance of *cEbf1* gene.



of HH17-18 chick embryos following implantation of DF-1 control cells (k, l) and Noggin expressing cells (m–p) medial to crPSM (m, n) and epithelial somites (o, p) show *cEbf1* expression. The blue arrowheads refer to the prospective site of the injected DF-1/Noggin cells and the green arrowheads indicate the prospective site of the injected cells. (q–v) Whole mount and transverse section of HH17-18 chick embryos following implantation of BMP4 loaded beads at different concentrations; 50 (q, r), 100 (s, t), and 150 µg/ml (u, v) show expression of *cEbf1*. In all photos, dashed lines indicate the site of transverse sections. Abbreviations: Ca, caudal; Cr, cranial; crPSM, cranial presomitic mesoderm; DM, dermomyotome; DSE, dorsal somitic epithelia; FP, floor plate; IM, intermediate mesoderm; LPM, lateral plate mesoderm; N, notochord; NT, neural tube; SI-SV, somites 1–5; Scl, sclerotome; Som, somitocoele; VSE, ventral somitic epithelia. Scale bars: c, e, g, k, m, o = 300 µm, q, s, u = 350 µm, d, f, h, l, n, p, r, t, v = 150 µm

To check whether inhibition of Bmp signaling in the medial somitic domain can also down-regulate *cEbf1* expression, Noggin secreting cells were injected medial to the crPSM or epithelial somites (arrowheads) and unexpectedly caused a complete down-regulation of *cEbf1* (Figure 5m,-Pp) as compared to control embryos (Figure 5k,l). On transverse sections, although Noggin implantation medial to the crPSM resulted in expansion of sclerotomal domain on the expense of the dermomyotomal domain, no *cEbf1* expression was seen in the entire sclerotome (Figure 5n).

In general, although inhibition of Bmps by Noggin injection induces sclerotomal cell formation, these cells failed to express *cEbf1* gene. This suggests that Bmp signals are crucial for both induction of *cEbf1* gene expression and maintenance of the identity of cells expressing *cEbf1* gene.

#### 2.2.4 Effect of ectopic expression of Bmp4 on *cEbf1* gene expression in somites

Our previous study has shown that Affigel beads soaked in recombinant Bmp4 protein at concentrations below the apoptotic threshold, for example, 50–200 µg/ml, are functionally active in the chick embryo (El-Magd et al., 2013). In this previous study, the accuracy and efficiency of the prepared Bmp4 beads as compared to control PBS beads were also confirmed.

In the present study, we checked the effect of gain of Bmp4 function on *cEbf1* expression by implanting beads soaked in Bmp4 protein into the crPSM. Implantation of Bmp4 beads (magenta arrowheads) at a lower concentration (50 µg/ml) resulted in not only up-regulation of *cEbf1* but also its ectopic expression in regions that normally did not express it (Figure 5q,r). For example, *cEbf1* was ectopically expressed in the ventrolateral domain (yellow arrowhead), the dorsomedial region of the intersomitic boundary (green arrowhead), and the caudal somitic half (white arrowhead, Figure 5q). Transverse sections showed *cEbf1* up-regulation in sclerotomal area adjacent to the NT (green arrowhead) and in the lateral sclerotomal domain which normally does not express *cEbf1* (yellow arrowhead, Figure 5r). In addition and as expected, the dermomyotome at the bead side was ill-developed as compared to the contralateral side.

To explore whether the concentration of Bmp4 is important for defining distinct domains of gene expression in the chick somitic mesoderm, and if *cEbf1* responds to alterations in the level of signaling, beads soaked in 100 and 150 µg/ml Bmp4 (still below the apoptotic threshold) were placed in the crPSM. At moderate Bmp4 concentration (100 µg/ml), *cEbf1* expression was lost in the central sclerotomal domain (green arrowhead), but remained weakly in the medial domain (yellow arrowhead, Figure 5s,t). When the concentration of Bmp4 protein increased to (150 µg/ml), *cEbf1* was abolished in the somites (Figure 5u,v).

In summary, these findings indicate that *cEbf1* positively respond to the exogenous Bmp4 protein at a lower concentration. However, the gradual increase in Bmp4 concentration leads to gradual reduction of *cEbf1*. This means that *cEbf1* expression is only increased by low dose of exogenous Bmp4 and is inhibited by higher doses.

## 2.3 Role of cEbf1 in mediolateral patterning of somite

### 2.3.1 Preparation of dominant negative Ebf1( $\Delta$ Ebf1) construct

To check the role of cEbf1 in the mediolateral patterning, we constructed a dominant-negative protein Ebf1 ( $\Delta$ Ebf1), using an RCAS retroviral vectors, by deleting the 321 bp corresponding to the 107N-terminal amino acids (e.g., TSI and portion of DBD of the full length mEbf1; Figure 6a). Similar construct derived from the *Xenopus Ebf2* gene was shown to have a dominant-negative activity (Dubois et al., 1998). Although, such a deletion retains a portion of DNA binding domain (from amino acids [aa] 108–251), dimerization domain and TSII domain, it has been shown previously to obliterate Ebf1 DNA-binding activity (Hagman, Belanger, Travis, Turck, & Grosschedl, 1993). Thus, it is likely that over-expressing this truncated protein would titrate the native cEbf1 and prevent its normal function via the formation of cEbf1– $\Delta$ mEbf1 DBD heterodimers that are not able to bind DNA properly. In these mis-expression experiments, mouse  $\Delta$ Ebf1 was used as the complete coding sequence of *mEbf1* is available and is highly homologous to chick *cEbf1*. Moreover, a similar mouse  $\Delta$ Ebf1 has been used successfully to mis-express cEbf1 during NT development (Garcia-Dominguez, Poquet, Garel, & Charnay, 2003). Additionally, the specificity of mouse  $\Delta$ Ebf1 to chick cells was further confirmed by the infection of chick DF-1 fibroblast cells with RCAS- $\Delta$ mEbf1 using anti-GAG staining. A high infection rate, revealed by intense brown coloration, was observed in RCAS- $\Delta$ mEbf1 infected DF-1 cells prior to viral harvest (Figure 6c) as compared to nontransfected control cells (Figure 6b).

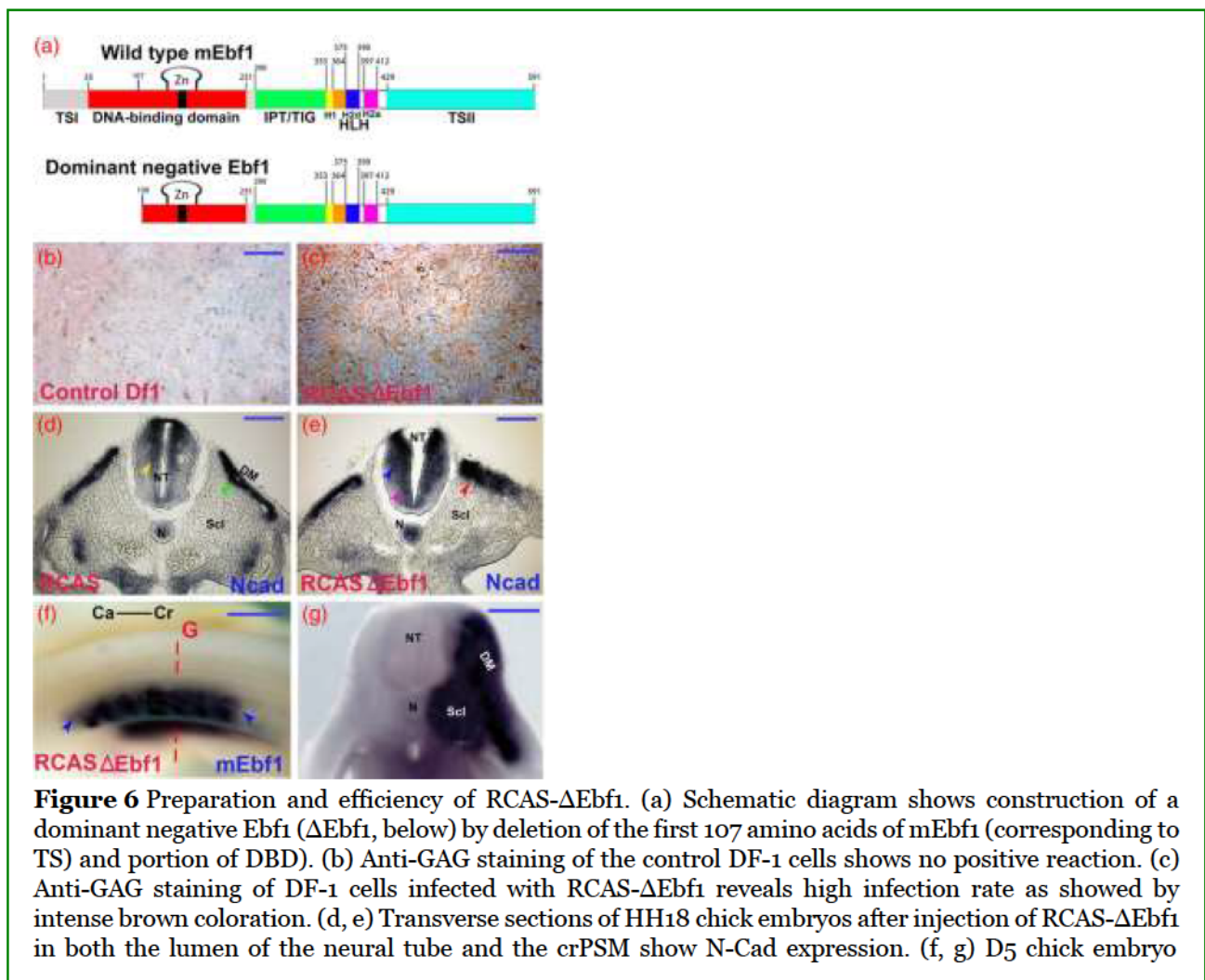


**Figure 6** Preparation and efficiency of RCAS- $\Delta$ Ebf1. (a) Schematic diagram shows construction of a dominant negative Ebf1 ( $\Delta$ Ebf1, below) by deletion of the first 107 amino acids of mEbf1 (corresponding to TS) and portion of DBD). (b) Anti-GAG staining of the control DF-1 cells shows no positive reaction. (c) Anti-GAG staining of DF-1 cells infected with RCAS- $\Delta$ Ebf1 reveals high infection rate as showed by intense brown coloration. (d, e) Transverse sections of HH18 chick embryos after injection of RCAS- $\Delta$ Ebf1 in both the lumen of the neural tube and the crPSM show N-Cad expression. (f, g) D5 chick embryo



following injection of RCAS- $\Delta$ mEbf1 in the crPSM shows *mEbf1* expression. In all photos, dashed lines indicate the site of transverse sections. Abbreviations: Ca, Caudal; Cr, cranial; DBD, DNA binding domain; DM, dermomyotome; H1 and H2a, ancestral helices; H2d, duplicated helix; HLH, helix-loop-helix; IPT/TIG, immunoglobulin-like plexins transcription factor; N, notochord; NT, neural tube; Scl, sclerotome; TSI, transactivation I; TSII, transactivation II; Zn, zinc finger motif. Scale bars: b, c = 50  $\mu$ m, d, e = 105  $\mu$ m, f = 350  $\mu$ m, g = 600  $\mu$ m

It has been reported that loss of cEbf1 function by over-expression of mouse  $\Delta$ Ebf1 can specifically up-regulate *N-Cad* expression in the NT of chick embryos (Garcia-Martinez & Schoenwolf, 1992). To prove that  $\Delta$ Ebf1 used in this study can efficiently inhibit the endogenous activity of cEbf1, RCAS- $\Delta$ Ebf1 was injected into both the crPSM and the lumen of the NT of HH9 chick embryos ( $n = 14$ ). Following  $\sim 48$  hr reincubation, alive embryos at stage HH17 ( $n = 12$ ) were fixed and analyzed by in situ hybridization using an *N-Cad* mRNA probe. As expected, expression of RCAS- $\Delta$ Ebf1 increased the expression domain of *N-Cad* both laterally (blue arrowhead) and ventrally (magenta arrowhead) in the NT (Figure 6e, 10 out of 12 embryos showed this altered expression while the other two embryos showed a very slight up-regulation). Likewise, the control embryos ( $n = 14$ ) which was injected with RCAS alone, showed normal expression of *N-Cad* in the ventricular layer of the dorsal portion of the NT (yellow arrowhead, Figure 6d, all harvested alive embryos ( $n = 12$ ) showed this expression). This confirms that  $\Delta$ Ebf1 used in this study can efficiently inhibit the endogenous activity of cEbf1. It is also notable that injection of RCAS- $\Delta$ Ebf1 in the crPSM resulted in up-regulation of *N-Cad* expression in the dermomyotome (red arrowhead, Figure 6e) compared to the control embryos (green arrowhead, Figure 6d). This injection also led to formation of dermomyotome bigger than the control one.

To confirm the infection with RCAS- $\Delta$ Ebf1 and to ascertain that the RCAS- $\Delta$ Ebf1 can consistently achieve high-level infection in the somites, the PSM of 5 HH9-10 embryos were injected with RCAS- $\Delta$ Ebf1, in order to infect the majority of somitic tissue *in ovo*, and embryos were harvested at Day 5 for whole mount in situ hybridization with an antisense riboprobe for *mEbf1*. The *mEbf1* was extensively expressed in the somites of all injected embryos (Figure 6f). Transverse section showed a robust expression of *mEbf1* in the sclerotome and the dermomyotome as well as weak expression ventral to aorta (Figure 6g). No expression was detected in the somite of the contralateral side. This extensive viral distribution along with up-regulation of *N-Cad* in the NT confirmed that RCAS- $\Delta$ Ebf1 produces high-level infection in the somites and any subsequent molecular changes should be due to  $\Delta$ Ebf1 misexpression, which was assumed to be loss of function as previously stated (Dubois et al., 1998; Garcia-Dominguez et al., 2003; Hagman et al., 1993).

To investigate the effect of  $\Delta$ Ebf1 misexpression/Ebf1 loss of function on the mediolateral patterning of somites, RCAS- $\Delta$ Ebf1 was injected into the PSM at stage HH9-10 and the medial sclerotomal marker, *cPax1*, the dermomyotomal marker with highest expression in the lateral dermomyotomal lips, *cPax3*, and the lateral sclerotomal marker, *cEbf3*, were analyzed by in situ hybridization (Figure 7).

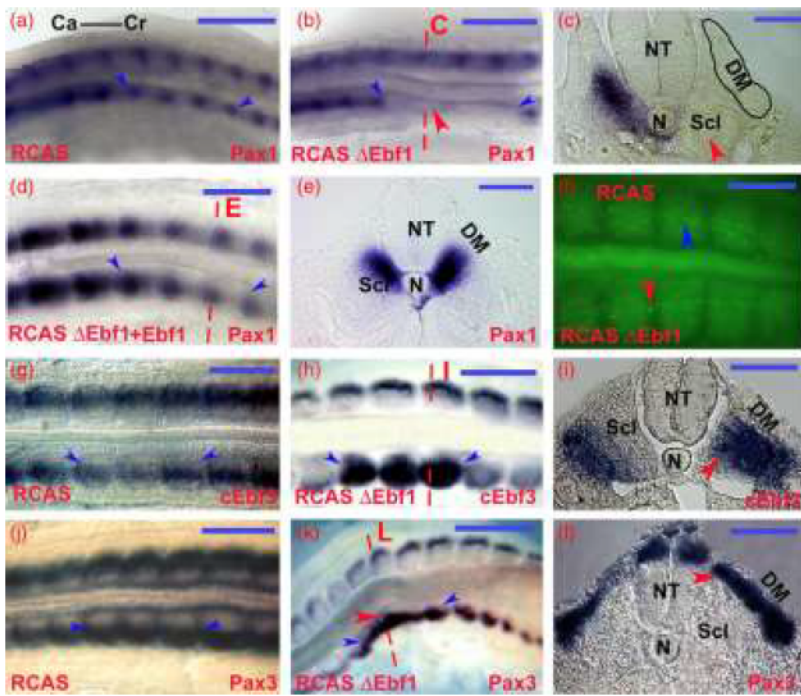


**Figure 7** Molecular analysis of  $\Delta Ebf1$  injected embryos. (a–e) Whole mount in situ hybridization and transverse sections (c, e) of HH15-16 chick embryos following injection of either RCAS (a), RCAS- $\Delta Ebf1$  (b), or RCAS- $\Delta Ebf1$ + Ebf1 (d) in the crPSM show *cPax1* expression. (f) Whole mount acridine orange staining of HH16 chick embryo following injection of RCAS (left side) and RCAS- $\Delta Ebf1$  (right side) in the crPSM shows a similar level of apoptotic cells in both sides (arrowheads). (g–l) Whole mount and transverse sections of HH15-16 chick embryos following injection of either RCAS (g, j) or RCAS- $\Delta Ebf1$  (h, k) in the crPSM show *cEbf3* (g–i) and *cPax3* (j–l). Regions between each two blue arrowheads refer to injection site. Abbreviations: DM, dermomyotome; N, notochord; NT, neural tube; Scl, sclerotome. Scale bars: a, b, h = 350  $\mu$ m; d, e, g, f = 250  $\mu$ m; c, i, j = 150  $\mu$ m

### 2.3.2 Inhibition of *cEbf1* completely down-regulates the medial sclerotomal marker, *cPax1*

We previously proved that *cEbf1* expression precedes *cPax1* in the somites (El-Magd et al., 2015) and both genes are downstream targets of the *Shh* signaling pathway (Christ, Huang, & Wilting, 2000; El-Magd et al., 2015). To determine whether *cEbf1* regulates *cPax1* expression, RCAS- $\Delta Ebf1$  was injected into the crPSM of HH9-10 chick embryos ( $n = 14$ ) which were then reincubated for 24 hr until stage HH15-16 (number of alive harvested embryos = 12). Analysis of *cPax1* expression in  $\Delta Ebf1$  injected embryos showed complete down-regulation of this expression in somites (red arrowhead, Figure 7b, in 10 embryos, while the other two embryos showed a slight reduction of *cPax1* expression) compared to control embryos injected with empty RCAS (Figure 7a, in all four alive harvested embryos). Transverse sections not only showed the complete loss of *cPax1* expression (red arrowhead) but also revealed normal epithelial mesenchymal transition, but with hypertrophied dermomyotome on the injected side compared to the contralateral noninjected side (Figure 7c). The lost *cPax1* expression was rescued when embryos were injected with RCAS- $\Delta Ebf1$  co-transfected with wild type Ebf1 (Figure 7d,e). These findings indicate that *cPax1* expression in the sclerotome lies downstream to, and is dependent on, the *cEbf1* activity.

The mechanism for down-regulation of *cPax1* was investigated by analyzing  $\Delta Ebf1$  embryos for changes in levels of cellular apoptosis. To identify whether down-regulation of *cPax1* is due to changes in cells fate or cells loss due to increased cell death, whole mount acridine orange staining was used to show apoptotic

cells. HH9 embryos ( $n = 15$ ) were injected with RCAS- $\Delta Ebf1$  and empty RCAS (control) in the right and left crPSM, respectively. Following incubation for 36 hr, the profile of apoptotic cells in  $\Delta Ebf1$  injected side (red arrowhead, Figure 7f, in all 12 alive harvested HH17 embryos) was similar to that seen in the control side (blue arrowhead, Figure 7f). This indicates that the loss of *cPax1* expression is not a secondary consequence of loss of a subset of sclerotomal cells, but it is rather a very early molecular defect caused by  $\Delta Ebf1$  misexpression/*Ebf1* loss function in the sclerotome.

### 2.3.3 Inhibition of *cEbf1* up-regulates the lateral sclerotomal marker, *cEbf3*

Since  $\Delta Ebf1$  misexpression/*Ebf1* loss function down-regulates the medial sclerotomal marker *cPax1*, it is also possible that  $\Delta Ebf1$  can change the cell fate of somitic tissues. To explore this, the effect of the RCAS- $\Delta Ebf1$  on the expression of a lateral sclerotomal marker, *cEbf3*, was checked. RCAS- $\Delta Ebf1$  was injected in the crPSM of HH9 embryos ( $n = 15$ ) and these were then fixed at stage HH16 (number of alive harvested embryos = 12). As expected, *cEbf3* expression was up-regulated in somites of the  $\Delta Ebf1$  embryos (red arrowheads, Figure 7h,i, in 10 embryos, while the other two embryos showed slight *cEbf3* up-regulation) as compared to the control embryos (Figure 7g, in all 12 harvested alive embryos). This medial expression of the lateral marker *cEbf3* indicates that the sclerotome becomes lateralized in absence of *Ebf1*.

### 2.3.4 *cEbf1* inhibition up-regulates the dermomyotomal *Pax3*

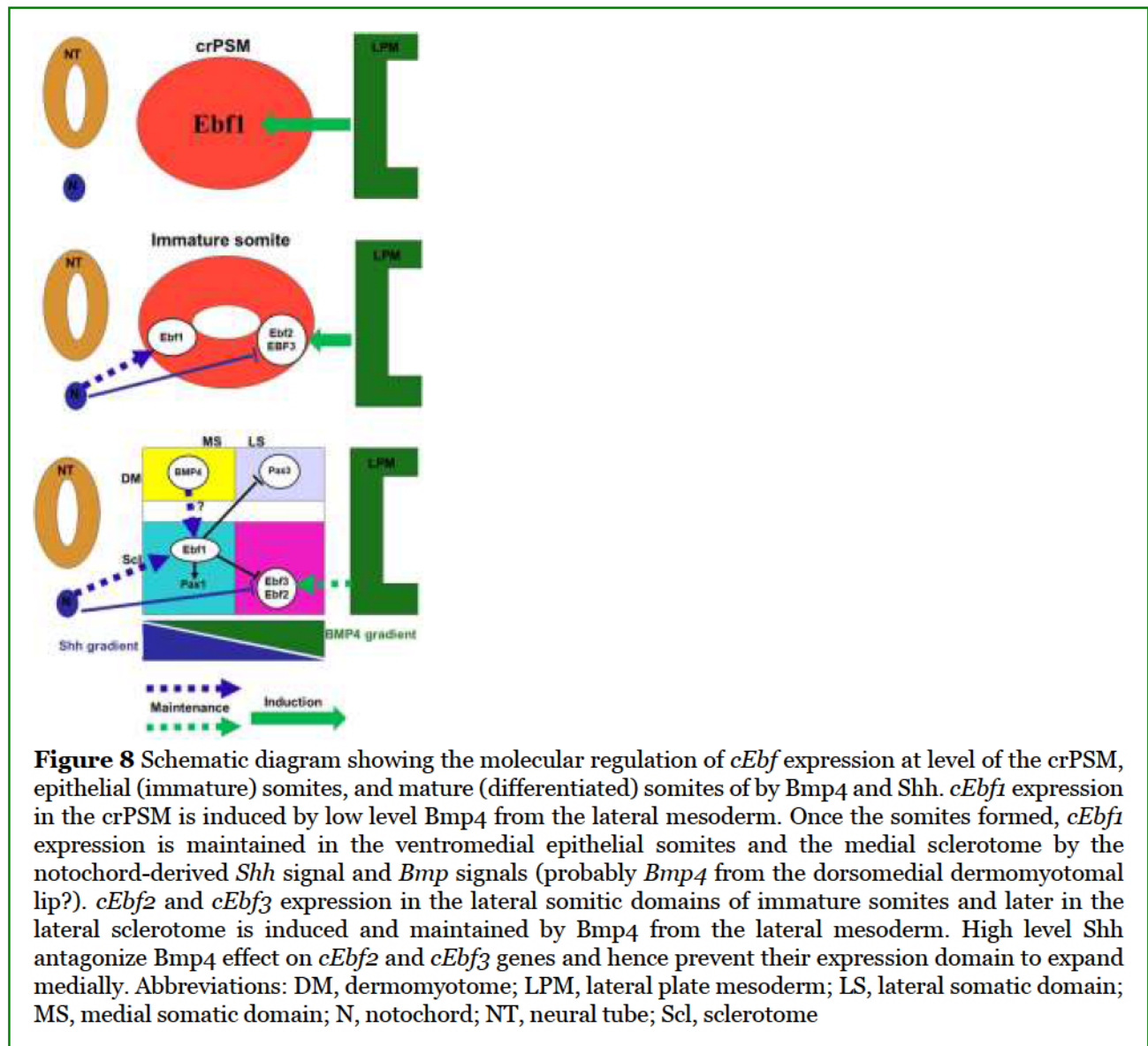
Complete loss of the medial sclerotomal marker *cPax1* and up-regulation of the lateral sclerotomal marker *cEbf3* following  $\Delta Ebf1$  misexpression/*Ebf1* loss function suggest that the medial cells may have adopted a lateral identity. Therefore, it is possible that mis-expression of  $\Delta Ebf1$  could also up-regulate *cPax3* (a dermomyotomal marker with highest expression in the lateral dermomyotomal lips). RCAS- $\Delta Ebf1$  or empty RCAS was injected into the crPSM of HH9 chick embryos and these were reincubated until reaching stage HH15. In control embryos ( $n = 5$ ), *cPax3* was localized mainly in the lateral dermomyotomal lips with only a very weak expression in the medial dermomyotomal lips (Figure 7j, in all four alive harvested embryos). In contrast,  $\Delta Ebf1$  injected embryos ( $n = 15$ ) showed up-regulation of *cPax3* in the medial and lateral domains of the dermomyotome (red arrowhead, Figure 7k,l, in 11 embryos, while the other one alive harvested embryo showed unremarkable up-regulation). This medial expansion of *cPax3* means that the somitic cells adopt a lateral fate and that *cEbf1* is crucial for maintenance of the medial identity of the somitic cells.

## 3 DISCUSSION

Our prior two studies revealed that *cEbf1* expression in the medial sclerotome is regulated by *Shh* signals from the notochord, while *cEbf2,3* expression in the lateral sclerotome is regulated by the lateral mesoderm-derived *Bmp4* signals (El-Magd et al., 2013, 2015). However, these two studies lacked some important information regarding: (a) the regulation of *cEbf1* early expression in the crPSM; (b) the effect of the lateral signals (mainly *Bmp4*) on the medial sclerotomal marker, *cEbf1*; (c) the effect of axial signals (mainly *Shh*) on the lateral sclerotomal markers, *cEbf2/3*; and (d) the role of *cEbf* genes in somites patterning (due to lack of loss and/or gain of function experiment on *cEbf* genes). Therefore, we conducted the present study to complete the previous work and to check whether *cEbf1* could be downstream targets in *Shh* and *Bmp4* signaling cascade regulating the mediolateral patterning of the somites.

The first gap addressed in the present study was the regulation of *cEbf1* early expression in the crPSM. Our previous study showed that *cEbf1* is expressed in the crPSM, but the tissues and signals regulating (by induction and/or maintenance) this expression have not been determined (El-Magd et al., 2015). Herein, we reported for the first time that the lateral mesodermal signals, but not the notochord signals, are the initial inducer of *cEbf1* expression in the crPSM and the notochord signals are mainly required for sclerotomal formation and hence maintenance of this expression (Figure 8). This overall conclusion was based on the finding that *cEbf1* expression can be induced in the crPSM in isolation from the notochord as insertion of a medial barrier at the level of caudal PSM followed by short incubation time resulted in only a slight reduction

of *cEbf1* expression in the crPSM. In contrast, isolation of the crPSM from the lateral mesoderm completely down-regulates *cEbf1* expression, suggesting induction of *cEbf1* expression by lateral signals. Following this type of operation, the sclerotomal cells are formed normally, and characterized by high rate of proliferation (Cheng, Alvares, Ahmed, El-Hanfy, & Dietrich, 2004; Dietrich et al., 1997), however *cEbf1* was not initiated in these cells. Unlike *cEbf1*, the domain of the medial sclerotomal marker *Pax1* was expanded following separation of the somitic mesoderm from the lateral mesoderm (Cheng et al., 2004; Dietrich et al., 1997). This suggests that *cEbf1* is a novel medial sclerotomal marker whose expression is induced by lateral signals. However, these lateral signals are not required for maintenance of *cEbf1* expression since this expression was maintained after insertion of the lateral barriers at the level of epithelial somites.



Tissue manipulations supported by *Shh* gain and loss of experiments in the present study and our previous study (El-Magd et al., 2015) indicate that notochord-derived *Shh* signals are necessary for maintenance of *cEbf1* expression in the ventromedial part of the immature (epithelial) somites and further in the medial sclerotomal domain (Figure 8). In parallel, *Shh* knock-out mice display close to normal, but transient, *Pax1* expression in the medial sclerotome, suggesting that *Shh* may act to maintain and/or expand the population of *Pax1*-positive cells, rather than induce these cells (Chiang et al., 1996). Furthermore, *Shh* as a mitogen, has the ability to completely rescue normal somite proliferation after separation of somites from axial structures

or after removal of notochord (Marcelle et al., 1999; Teillet et al., 1998). Therefore, *Shh* might serve to expand a population of *cEbf1*-positive cells induced by factor(s) emanating from the lateral plate, most likely *Bmp2/4*.

Therefore, the second issue addressed in the present study was whether *Bmp4* is the lateral signal that induces *cEbf1* expression in the somites. In support of this idea, inhibition of *Bmps* by implantation of *Noggin*-expressing cells between crPSM and either axial or lateral structures downregulated *cEbf1* and ectopic overexpression of low dose of *Bmp4* in the crPSM upregulated *cEbf1*. Thus, *Bmp4* is the lateral mesoderm-derived signal that induces *cEbf1* expression in crPSM and epithelial somites (Figure 8). Unlike the results obtained from the lateral barrier insertion which revealed no effect for the lateral signals on maintenance of *cEbf1* expression in the medial sclerotome, results from loss of *Bmp* function showed that ectopic *noggin* (*Bmp* antagonist) between the epithelial somites and the NT completely reduces *cEbf1* expression. This indicates that *Bmp* required for maintenance of medial *cEbf1* expression is not derived from lateral tissues. The roof plate of the NT and the overlying ectoderm are further two sources of *Bmp4* signals (Monsoro-Burq, 2005; Monsoro-Burq & Le Douarin, 2000). This dorsal *Bmp4* is unlikely to have a regulatory effect on *cEbf1* expression as ablation of ectoderm (data not shown) or NT does not change *cEbf1* expression, and dorsal *Bmp4* signals mainly target the dorsal somitic cells to negatively regulate epaxial myogenesis (Sela-Donenfeld & Kalcheim, 2002). Therefore, it is possible that the *Bmp* source for maintaining medial *cEbf1* expression may be intrinsic (from the somites). In agreement with this notion, *Bmp2/4* and *smad1* (*Bmp* activator) are expressed in the dorsomedial dermomyotomal lip at HH11-13 stage (Danesh et al., 2009; Faure, de Santa Barbara, Roberts, & Whitman, 2002), the same stage as microsurgical manipulations and *Noggin* injections were performed in this study. Thus, it is possible that these medial intrinsic *Bmps* may maintain *cEbf1* expression in medial somitic domain (Figure 8). To check this possibility, tissue ablation experiments by removing the dermomyotome domain alone is required to check whether *cEbf1* expression will be maintained or not. Overall, it is conceivable that an initial lateralizing signal conveyed by *Bmp4* produces a plastic polarity in the somite, and that axial signals (*Shh*), coming later, fix and elaborate the polarity.

Regarding regulation of *cEbf2* and *cEbf3* expression in the somites, our previous study revealed that lateral mesoderm derived-*Bmp4* signal induces and maintains this expression (El-Magd et al., 2013). However, in this previous work, the effect of notochord signals (*Shh* and *Noggin*) on *cEbf2* and *cEbf3* expression was not investigated. Again, this third gap was addressed in the present study. Previous studies have indicated that notochord removal results in up-regulation of the lateral somitic marker, *Sim1*, which is expressed first in the entire lateral half of the epithelial somite, and further localized in the lateral dermomyotome and sclerotome) (Christ et al., 2000; Dockter, 2000). Consistent with this, ectopic *cEbf3* expression is induced in the medial sclerotomal domain following isolation of somitic mesoderm from axial structures by notochord removal or medial barrier implantation. This suggests that the notochord produces signal to antagonize *cEbf3* expression and thus blocks *cEbf3* in medial somite. This signal is unlikely to be *Shh* because inhibition of *Shh* by cyclopamine does not affect *cEbf2* and *cEbf3* expression. On the other hand, although ectopic application of *Shh* inhibits this expression in a dose-dependent manner (with a low dose [0.5 µg/µl], the expression remained normal, with a moderate dose [1 µg/µl], the expression became slightly reduced, with a high dose [2 µg/µl], the expression was completely extinguished), this change may be secondary to change in identity of the cells after over-expression of *Shh*, that is, the lateral sclerotomal cells were respecified to be medial cells and hence *cEbf2* and *cEbf3* expression was lost. Similarly, previous studies have indicated that relatively high concentrations of *Shh* maintain the expression of the sclerotomal markers (*Pax1*, *Nkx3.2*, and *Sox9*; Cairns et al., 2008; Chiang et al., 1996) and repress the dermomyotomal markers (*Pax3* and *Pax7*; Hammond et al., 2007) through medialization of somitic cells. Taken together, *Shh* is not the notochordal signal that directly inhibits *cEbf3* expression. It is likely that another molecule from the notochord is required to antagonize *Bmp4* and so inhibits expression of *cEbf3* medially. A good candidate gene with these criteria is *Noggin*, since it is a medial signal secreted from the notochord (McMahon et al., 1998) and acts either synergistically with *Shh* to activate medial sclerotomic markers, such as *Pax1* (Dockter & Ordahl, 2000) or alone to inhibit the lateralization effect of lateral mesoderm signals, especially *Bmp4* (Tonegawa & Takahashi, 1998). In agreement, *Noggin* over-expression in the lateral PSM results in complete loss of *cEbf2* and *cEbf3* (El-Magd et al., 2013).

Before this study, there is no definitive work studying the ML molecular identity of the sclerotome. Although, we have previously found that the expression domains of *cEbf1* and *cEbf2, 3* molecularly define the medial and the lateral portion of the sclerotome, respectively (El-Magd et al., 2013, 2015), the actual function

of *cEbf* genes during mediolateral patterning of somites was not determined due to lack of Ebf gain and loss of function experiment. Again, this fourth gap was addressed in the present study. Mis-expression of  $\Delta Ebf1$ , which probably causes cEbf1 loss of function (Dubois et al., 1998; Garcia-Dominguez et al., 2003; Hagman et al., 1993), revealed a possible significant role for cEbf1 in maintenance of medial somite identity (Figure 8). When  $\Delta Ebf1$  mis-expressed, the medial sclerotome marker *cPax1* was completely down-regulated and the somite assumed a lateral identity as revealed by up-regulation of the lateral dermomyotome marker *cPax3* and the lateral sclerotome marker *cEbf3*. This suggests that cEbf1 may be a potential determinant of medial somite identity. Therefore, cEbf1 may be necessary for commitment (specification) of somitic precursor to a sclerotomal fate because its inhibition results in complete loss of *Pax1* which is the key regulator for sclerotomal induction and specification (Borycki et al., 1998; Christ, Huang, & Scaal, 2004; Dockter & Ordahl, 2000; Peters et al., 1999; Rodrigo, Hill, Balling, Munsterberg, & Imai, 2003). This means that the developmental function of cEbf1 may be required for directing the medial somite to form sclerotome. Further investigations are required to identify whether *cEbf1* can directly induce *Pax1* by binding to its promoter or indirectly by maintaining the identity of its expressing cells.

The classical model depicting the ML patterning of the somite indicates that Bmp4 is only needed for lateralization of somites and should be completely inhibited, by Noggin, in the medial domain to keep the ML identity (Danesh et al., 2009; Hirsinger et al., 1997; Nowicki, Takimoto, & Burke, 2003; Pourquie et al., 1995, 1996; Stafford et al., 2011, 2014; Stern & Piatkowska, 2015; Tonegawa et al., 1997). In these studies, Bmp signaling was not manipulated at a very low concentration. This prompts us to check the effect of different Bmp concentration. Indeed, we have found that a differential concentration of Bmp4 is required along the ML axis of somitic mesoderm to keep the medial and lateral identity of *cEbf* expressing sclerotomal cells. Moderate and high Bmp4 levels favor for the formation of lateral sclerotome may be through activation of the lateral markers *cEbf2*, *3* and inhibition of the medial sclerotomal marker *cEbf1*. However, a lower level is required for establishment of the medial somitic domain via activation of *cEbf1*. Loss of the medial sclerotomal markers caused by moderate and high level of the Bmp4 raised two possibilities: (a) the cells that would normally contribute to the medial sclerotome died in response to Bmp4, or (b) these cells survived but were transformed to another cell type. The first possibility is unlikely because Bmp4 was used at concentrations below levels that normally induce apoptosis. In agreement with the second possibility, moderate and high doses of Bmp4 lateralized the somites, that is, the medial sclerotomal cells expressing *cEbf1* transformed into lateral sclerotomal cells expressing *cEbf2* and *cEbf3*. This also indicates that only low levels of Bmp4 are able to keep the identity of medial sclerotomal cells. The pattern and timing of Bmp signaling along the ML axis of the embryo, as revealed by phosphorylated Smad1 activity (Faure et al., 2002), are consistent with the current finding that low doses of Bmp signaling pattern the medial somites. At stages HH11-13, phosphorylated Smad1 is detectable strongly within the lateral plate mesoderm, moderate in the lateral somites, and weakly in the medial somites. These findings are novel and disagree with the old model for ML patterning. Therefore, the old theory for influence of Noggin and Bmp on the ML identity within somites should be revised. We propose a model for regulation of *cEbf* genes in the somitic mesoderm along the ML axis during normal embryogenesis (Figure 8). Bmp4 induces *cEbf* genes expression in the crPSM and immature somites. Subsequently, the mature somite acquires ML polarity: the lateral portion expressing *cEbf2* and *cEbf3* is established by high Bmp4 and the medial one expressing *cEbf1* is formed by high Shh and low Bmp4. This means that both Shh and Bmp4 regulate *cEbf* expression in somites in a morphogen-like fashion but in opposite directions. However, in the absence of any information on the concentration of Bmp4 and Shh proteins that diffuse out of the beads, estimation of the effective dose of these two proteins remains speculative. Another problem of using bead experiments is that the obtained effect may be attributed to the duration of exposure rather than the concentration (dose-response). For example, at lower concentrations the protein may run out of the bead quicker. Therefore, further in vitro studies (somite explant culture) are recommended to accurately estimate the effect of different concentrations and duration of Bmp4 and Shh on *Ebf* genes expression.

Striking similarities exist between mammalian and avian EBF expression in the somites, where both chick (El-Magd et al., 2013, 2015) and mouse *Ebf* genes (Garel et al., 1997; Kieslinger et al., 2005) are expressed in medial (*Ebf1*) and lateral (*Ebf2* and *Ebf3*) sclerotomal domains. This therefore suggests a common evolutionary conserved role for these genes in patterning of the somite along the ML axis. In anamniotes, *Xenopus xEbf2, 3* and zebrafish *zEbf2, 3* have similar lateral somitic expression as their amniote counterparts (Dubois et al., 1998). Moreover, the cephalochordate EBF in *Amphioxus*, *AmphiCoe*, is notably expressed in

the mesoderm at the extremely lateral portion of the mature somites and in the adjacent lateral mesoderm (Mazet, Masood, Luke, Holland, & Shimeld, 2004). This suggests that the vertebrate ancestors of EBF expressing cells originally resided in the lateral somitic/lateral mesoderm interface. This could also explain why all *cEbf* genes are controlled by Bmp4 from the lateral mesoderm.

## 4 CONCLUSION

To the best of our knowledge, this may be the first study to demonstrate that *cEbf1* plays a critical role in mediolateral patterning of somites. As a specific medial sclerotomal marker, *cEbf1* induces the medial sclerotomal marker, *Pax1*, and antagonizes the lateral sclerotomal marker *cEbf3* and the dermomyotomal marker (with abundant lateral expression) *cPax3*. Its expression is maintained by Shh from the notochord. However, unlike all other known medial markers, *cEbf1* expression in the medial somitic domain is induced by low levels of the lateral plate derived Bmp4. The other two chick *Ebf* genes, which act as lateral sclerotomal markers (especially *cEbf3*) are induced and maintained by Bmp4 and inhibited by high dose of Shh. This indicates that Bmp4 activity is required along the ML axis of the somites. These striking findings are novel and give a new insight on the role of Bmp on ML patterning of somites through regulation of *Ebf* genes expression.

## 5 MATERIALS AND METHODS

### 5.1 Embryo preparation

Fertile hens' eggs were incubated at 38°C, 80% relative humidity to give embryos at stages HH9-D5 (Hamburger & Hamilton, 1951).

### 5.2 Embryo manipulations

All microsurgeries were performed on chick embryos at HH11-13 when the PSM is at its maximum length, ensuring the largest target area possible. Therefore, all induction experiments for *cEbf1* were carried out on a large area of crPSM about 5–9 somites length. Manipulations were performed at both crPSM (either during or prior to initiation of *cEbf1* or *cEbf2*, 3 expression, respectively) and epithelial somite level (after induction of *cEbf* expression) to isolate the tissues both inducing and maintaining expression of *cEbf* genes, respectively. This was achieved by either insertion of impermeable barriers or ablation of candidate tissues.

#### 5.2.1 Barrier insertion

A thin Nile blue stained tungsten needle (STN) was used to make a slit of 5–8 somites length either medially between the paraxial mesoderm (epithelial somites or crPSM) and the NT or laterally between the paraxial mesoderm and lateral mesoderm. This slit was then deepened inwardly to the notochord and a piece of thin, sterilized aluminum foil was rapidly inserted. Following barrier insertion, excess PBS was removed from the embryo using tissue paper thus sealing the slit.

#### 5.2.2 Axial structure removal

The NT and notochord were separated from the paraxial mesoderm using a STN then two transverse incisions were made at the anterior and posterior ends of the NT/notochord segment and the ablated segment rapidly removed from the egg.

#### 5.2.3 Neural tube removal

A gap between the NT and crPSM on both the left and right sides of the NT were made using STN. A caudal transverse incision was made in the NT, and the NT was raised with STN in a caudal to cranial direction. The floor of the NT was carefully separated from the underlying notochord then a transverse incision was made through the NT at the cranial end of the operation region releasing the NT from the embryo.

#### 5.2.4 Application of cyclopamine and beads

Application of cyclopamine and beads were performed as previously described (El-Magd et al., 2013, 2015; El-Magd, Saleh, El-Aziz, & Salama, 2014).

### 5.3 Preparation and injection of RCAS-dominant negative Ebf1 ( $\Delta$ Ebf1)

The retrovirus RCASBP(A) was used to express dominant negative Ebf1 ( $\Delta$ Ebf1) protein in the chick embryo somites using the same strategy as described by (Morgan & Fekete, 1996) and as summarized in the Figure S1. Briefly, an expression plasmid containing full length mouse mEbf1 was obtained as a gift from Prof. Roessler et al. (2007). The  $\Delta$ Ebf1 coding sequence used in this study was constructed by deletion of the 5' 321 bp of coding sequence corresponding to the N-terminal 107 aa using polymerase chain reaction (PCR) with the following two primers: a 5' primer CATGCCATGGTCCACTACCGGCTCCAGCTC with a Nco1 restriction site (CCATGG) preceding codon 108 (TCC) and a 3' primer GATCGAATTCTCACATGGGAGGGACAATCATATGC that spanned the stop codon (TCA) followed by an EcoRI restriction site (GAATTC). This truncation is corresponding to both N-terminal transactivation domain (from aa 1 to 34) and portion of DNA binding domain (from aa 35 to 107). A proofreading DNA polymerase, Pfu (Promega) was used to minimize errors during the PCR. The PCR product of the truncated *mEbf1* (1.455 kb) was cut by Nco1 and EcoRI into large Nco1-NcoI fragment (1.248 kb) and small NcoI-EcoRI fragment (0.207 kb). The two fragments were separately cloned into Slax12Nco adaptor plasmid, where the smaller fragment was ligated first then the larger one, following the standard cloning procedures. Because it is two piece cloning, orientation of the insert was verified by KpnI, which cuts at two unique sites; one 3' to the insert in Slax12 Nco and the other 0.890 Kb into the insert sequence to give either a 0.980Kb fragment for correct direction or a 0.893Kb fragment for incorrect orientation. These clones were sequenced (Geneservice, Cambridge, UK) to ensure that no mutations occurred during PCR as well as to confirm correct orientation. The entire  $\Delta$ Ebf1 fragment was then excised by digestion with ClaI. The ClaI-ClaI fragment of Slax12Nco- $\Delta$ Ebf1 was cloned into RCASBP(A) (ClaI digested and dephosphorylated by alkaline phosphatase) and digested with EcoRV to confirm the orientation of the insert. Characteristic bands of 5.121 and 0.823 kb are produced from the correct orientation and 3.041 and 2.543 kb fragments from the incorrect orientation.

Virus was generated according to protocols described by (Morgan & Fekete, 1996). In brief, once the RCAS vector has been built and a clone with the correct insert orientation has been selected, the proviral vector is amplified as bacterial plasmid to generate large quantities of proviral DNA. This DNA is then transfected into chicken embryo fibroblast cell line, DF1 (CRL-12203), using standard in vitro techniques to generate producer cells, in which active virus forms (virions) are shed into the culture medium. The supernatant containing infectious virions was collected and the virus harvested and then concentrated to yield high-titre viral stocks. The majority of embryos were injected at stage HH9-10. A small window in the egg shell was opened and the axis of the embryo was oriented to be parallel to the micropipette with the tail closest to the needle. The needle was inserted in the crPSM, under the ectodermal layer labeled by Nile blue stain, and about 0.1  $\mu$ l viral stock ( $1 \times 10^8$ ) was slowly injected as previously described (Morgan & Fekete, 1996).

#### 5.4 Anti-GAG immunostaining of virally infected DF-1 cells

The infection of chick DF-1 cells with RCASBP- $\Delta$ Ebf1 was monitored using 3C2 hybridoma supernatant mouse-anti-GAG staining. Briefly, cells were rinsed with PBS, fixed with 4% PFA (15–30 min, at room temperature) washed with PBS (15 min) and pre-blocked in the blocking solution (DMEM media containing 10% fetal bovine serum [FBS], 0.05% Triton X-100) for 1 hr. The cells were incubated in 3C2 antibody (diluted



1:4 in DMEM containing 10% FBS plus 0.05% Triton X-100, 30 min before using) for 1 hr at room temperature (RT). After rinsing twice in PBS, the cells were incubated in Biotin conjugated Rabbit anti-mouse IgG, IgM, secondary antibody (diluted 1:200 in blocking solution at least 30 min prior to use) for at least 30 min at RT. Following rinsing with PBS, avidin and biotinylated horseradish peroxidase macromolecular complex reagent (made 30 min before use, using 20 µl of A and B in 2 ml PBS) was added and samples incubated for 30 min at RT. After rinsing twice in PBS, the cells were washed 15 min in distilled water. Color was developed for 2–5 min in dark at RT using Diamino Benzidine as a substrate. The reaction was stopped by rinsing several times with water. When infection was 50% or higher cells were transferred into bigger flask (T75) for further processing.

## 5.5 Whole mount in situ hybridization

Harvested embryos were washed in PBS and fixed in 4% paraformaldehyde, overnight at 4°C. Whole-mount in situ hybridization using DIG-labeled RNA probes was performed as described previously (Nieto, Patel, & Wilkinson, 1996). Chick probes used were: *cEbf1*, 696 bp; *cEbf2*, 405 bp; *cEbf3*, 504 bp (El-Magd et al., 2014); *mEbf1* 696 bp (kind gift of Prof. Grosschedl); *cN-Cad* (kind gift of Prof. Anthony Graham); *cPax3* (Otto, Schmidt, & Patel, 2006); and *cPax1* (kind gift of Prof. Bodo Christ). Whole mount embryos and sections were photographed as previously described (El-Magd et al., 2013).

## 5.6 Apoptosis

Fresh embryos were stained with acridine orange (AO) by diluting a stock solution of 1 mg/ml AO with PBS to give a working concentration of 0.1 µg/ml. Embryos were stained for approximately 5 min then briefly washed twice in PBS to remove the excess dye. After staining, embryos were covered with a cover slip and observed with a Leica confocal microscope (TCS SP5). AO shows selective affinity for chromatin of apoptotic cells, resulting in bright fluorescence.

## CONFLICT OF INTEREST

The authors declare that there is no conflict of interest regarding the publication of this article.

## AUTHOR CONTRIBUTIONS

M.E., I.M., S.A., and K.P. designed the experiments; M.E., S.E., E.E., A.A., and A.S. conducted the experiments; S.E. and E.E. helped with in situ hybridization; M.E., S.E., E.E., I.M., S.A., and K.P. analyzed the data; M.E., A.A., and A.S. wrote the manuscript; and all authors revised the manuscript.

## REFERENCES

- Borycki, A. G., Mendham, L., & Emerson, C. P., Jr. (1998). Control of somite patterning by sonic hedgehog and its downstream signal response genes. *Development*, **125**, 777–790.
- Cairns, D. M., Sato, M. E., Lee, P. G., Lassar, A. B., & Zeng, L. (2008). A gradient of Shh establishes mutually repressing somitic cell fates induced by Nkx3.2 and Pax3. *Developmental Biology*, **323**, 152–165.
- Cheng, L., Alvares, L. E., Ahmed, M. U., El-Hanfey, A. S., & Dietrich, S. (2004). The epaxial-hypaxial subdivision of the avian somite. *Developmental Biology*, **274**, 348–369.

- Chiang, C., Litingtung, Y., Lee, E., Young, K. E., Corden, J. L., Westphal, H., & Beachy, P. A. (1996). Cyclopia and defective axial patterning in mice lacking sonic hedgehog gene function. *Nature*, **383**, 407–413.
- Christ, B., Huang, R., & Scaal, M. (2004). Formation and differentiation of the avian sclerotome. *Anatomy and Embryology*, **208**, 333–350.
- Christ, B., Huang, R., & Wilting, J. (2000). The development of the avian vertebral column. *Anatomy and Embryology*, **202**, 179–194.
- Cordero, D., Marcucio, R., Hu, D., Gaffield, W., Tapadia, M., & Helms, J. A. (2004). Temporal perturbations in sonic hedgehog signaling elicit the spectrum of holoprosencephaly phenotypes. *The Journal of Clinical Investigation*, **114**, 485–494.
- Crozatier, M., Valle, D., Dubois, L., Ibnsouda, S., & Vincent, A. (1996). Collier, a novel regulator of *Drosophila* head development, is expressed in a single mitotic domain. *Current Biology*, **6**, 707–718.
- Danesh, S. M., Villasenor, A., Chong, D., Soukup, C., & Cleaver, O. (2009). BMP and BMP receptor expression during murine organogenesis. *Gene Expression Patterns*, **9**, 255–265.
- Dietrich, S., Schubert, F. R., & Lumsden, A. (1997). Control of dorsoventral pattern in the chick paraxial mesoderm. *Development*, **124**, 3895–3908.
- Dockter, J., & Ordahl, C. P. (2000). Dorsoventral axis determination in the somite: A re-examination. *Development*, **127**, 2201–2206.
- Dockter, J. L. (2000). Sclerotome induction and differentiation. *Current Topics in Developmental Biology*, **48**, 77–127.
- Dubois, L., Bally-Cuif, L., Crozatier, M., Moreau, J., Paquereau, L., & Vincent, A. (1998). X $Coe2$ , a transcription factor of the *col/Olf-1/EBF* family involved in the specification of primary neurons in *Xenopus*. *Current Biology*, **8**, 199–209.
- El-Magd, M., Saleh, A., El-Aziz, R. A., & Salama, M. (2014). The effect of RA on the chick *Ebf1-3* genes expression in somites and pharyngeal arches. *Development Genes and Evolution*, **224**, 245–253.
- El-Magd, M. A., Allen, S., McGonnell, I., Mansour, A. A., Otto, A., & Patel, K. (2015). Shh regulates chick *Ebf1* gene expression in somite development. *Gene*, **554**, 87–95.
- El-Magd, M. A., Allen, S., McGonnell, I., Otto, A., & Patel, K. (2013). *Bmp4* regulates chick *Ebf2* and *Ebf3* gene expression in somite development. *Development, Growth & Differentiation*, **55**, 710–722.

- El-Magd, M. A., Saleh, A. A., Farrag, F., Abd El-Aziz, R. M., Ali, H. A., & Salama, M. F. (2014). Regulation of chick ebf1-3 gene expression in the pharyngeal arches, cranial sensory ganglia and placodes. *Cells, Tissues, Organs*, **199**, 278–293.
- El-Magd, M. A., Sayed-Ahmed, A., Awad, A., & Shukry, M. (2014). Regulation of chick early B-cell factor-1 gene expression in feather development. *Acta Histochemica*, **116**, 577–582.
- Faure, S., de Santa Barbara, P., Roberts, D. J., & Whitman, M. (2002). Endogenous patterns of BMP signaling during early chick development. *Developmental Biology*, **244**, 44–65.
- Garcia-Dominguez, M., Poquet, C., Garel, S., & Charnay, P. (2003). Ebf gene function is required for coupling neuronal differentiation and cell cycle exit. *Development*, **130**, 6013–6025.
- Garcia-Martinez, V., & Schoenwolf, G. C. (1992). Positional control of mesoderm movement and fate during avian gastrulation and neurulation. *Developmental Dynamics*, **193**, 249–256.
- Garel, S., Marin, F., Mattei, M. G., Vesque, C., Vincent, A., & Charnay, P. (1997). Family of Ebf/Olf1-related genes potentially involved in neuronal differentiation and regional specification in the central nervous system. *Developmental Dynamics*, **210**, 191–205.
- Hagman, J., Belanger, C., Travis, A., Turck, C. W., & Grosschedl, R. (1993). Cloning and functional characterization of early B-cell factor, a regulator of lymphocyte-specific gene expression. *Genes & Development*, **7**, 760–773.
- Hamburger, V., & Hamilton, H. L. (1951). A series of normal stages in the development of the chick embryo. *Journal of Morphology*, **88**, 49–92.
- Hammond, C. L., Hinitz, Y., Osborn, D. P., Minchin, J. E., Tettamanti, G., & Hughes, S. M. (2007). Signals and myogenic regulatory factors restrict pax3 and pax7 expression to dermomyotome-like tissue in zebrafish. *Developmental Biology*, **302**, 504–521.
- Hirsinger, E., Duprez, D., Jouve, C., Malapert, P., Cooke, J., & Pourquie, O. (1997). Noggin acts downstream of Wnt and sonic hedgehog to antagonize BMP4 in avian somite patterning. *Development*, **124**, 4605–4614.
- Incardona, J. P., Gaffield, W., Kapur, R. P., & Roelink, H. (1998). The teratogenic Veratrum alkaloid cyclopamine inhibits sonic hedgehog signal transduction. *Development*, **125**, 3553–3562.
- Kieslinger, M., Folberth, S., Dobreva, G., Dorn, T., Croci, L., Erben, R., ... Grosschedl, R. (2005). EB1F2 regulates osteoblast-dependent differentiation of osteoclasts. *Developmental Cell*, **9**, 757–767.

- Marcelle, C., Ahlgren, S., & Bronner-Fraser, M. (1999). In vivo regulation of somite differentiation and proliferation by sonic hedgehog. *Developmental Biology*, **214**, 277–287.
- Mazet, F., Masood, S., Luke, G. N., Holland, N. D., & Shimeld, S. M. (2004). Expression of *AmphiCoe*, an amphioxus COE/EBF gene, in the developing central nervous system and epidermal sensory neurons. *Genesis*, **38**, 58–65.
- McMahon, J. A., Takada, S., Zimmerman, L. B., Fan, C. M., Harland, R. M., & McMahon, A. P. (1998). Noggin-mediated antagonism of BMP signaling is required for growth and patterning of the neural tube and somite. *Genes & Development*, **12**, 1438–1452.
- Mella, S., Soula, C., Morello, D., Crozatier, M., & Vincent, A. (2004). Expression patterns of the *coe/ebf* transcription factor genes during chicken and mouse limb development. *Gene Expression Patterns*, **4**, 537–542.
- Monsoro-Burq, A. H. (2005). Sclerotome development and morphogenesis: When experimental embryology meets genetics. *The International Journal of Developmental Biology*, **49**, 301–308.
- Monsoro-Burq, A. H., & Le Douarin, N. (2000). Duality of molecular signaling involved in vertebral chondrogenesis. *Current Topics in Developmental Biology*, **48**, 43–75.
- Morgan, B. A., & Fekete, D. M. (1996). Manipulating gene expression with replication-competent retroviruses. *Methods in Cell Biology*, **51**, 185–218.
- Moruzzo, D., Nobbio, L., Sterlini, B., Consalez, G. G., Benfenati, F., Schenone, A., & Corradi, A. (2017). The transcription factors EBF1 and EBF2 are positive regulators of myelination in Schwann cells. *Molecular Neurobiology*, **54**, 8117–8127.
- Nieto, M. A., Patel, K., & Wilkinson, D. G. (1996). In situ hybridization analysis of chick embryos in whole mount and tissue sections. *Methods in Cell Biology*, **51**, 219–235.
- Nowicki, J. L., Takimoto, R., & Burke, A. C. (2003). The lateral somitic frontier: Dorso-ventral aspects of antero-posterior regionalization in avian embryos. *Mechanisms of Development*, **120**, 227–240.
- Olivera-Martinez, I., Missier, S., Fraboulet, S., Thélu, J., & Dhouailly, D. (2002). Differential regulation of the chick dorsal thoracic dermal progenitors from the medial dermomyotome. *Development*, **129**, 4763–4772.
- Ordahl, C. P., & Le Douarin, N. M. (1992). Two myogenic lineages within the developing somite. *Development*, **114**, 339–353.

- Otto, A., Schmidt, C., & Patel, K. (2006). Pax3 and Pax7 expression and regulation in the avian embryo. *Anatomy and Embryology*, **211**, 293–310.
- Peters, H., Wilm, B., Sakai, N., Imai, K., Maas, R., & Balling, R. (1999). Pax1 and Pax9 synergistically regulate vertebral column development. *Development*, **126**, 5399–5408.
- Pourquie, O., Coltey, M., Breant, C., & Le Douarin, N. M. (1995). Control of somite patterning by signals from the lateral plate. *Proceedings of the National Academy of Sciences of the United States of America*, **92**, 3219–3223.
- Pourquie, O., Fan, C. M., Coltey, M., Hirsinger, E., Watanabe, Y., Breant, C., ... Le Douarin, N. M. (1996). Lateral and axial signals involved in avian somite patterning: A role for BMP4. *Cell*, **84**, 461–471.
- Psychoyos, D., & Stern, C. D. (1996). Fates and migratory routes of primitive streak cells in the chick embryo. *Development*, **122**, 1523–1534.
- Rodrigo, I., Hill, R. E., Balling, R., Munsterberg, A., & Imai, K. (2003). Pax1 and Pax9 activate Bapx1 to induce chondrogenic differentiation in the sclerotome. *Development*, **130**, 473–482.
- Roessler, S., Gyory, I., Imhof, S., Spivakov, M., Williams, R. R., Busslinger, M., ... Grosschedl, R. (2007). Distinct promoters mediate the regulation of Ebf1 gene expression by interleukin-7 and Pax5. *Molecular and Cellular Biology*, **27**, 579–594.
- Schoenwolf, G. C., Garcia-Martinez, V., & Dias, M. S. (1992). Mesoderm movement and fate during avian gastrulation and neurulation. *Developmental Dynamics*, **193**, 235–248.
- Seike, M., Omatsu, Y., Watanabe, H., Kondoh, G., & Nagasawa, T. (2018). Stem cell niche-specific Ebf3 maintains the bone marrow cavity. *Genes & Development*, **32**, 359–372.
- Sela-Donenfeld, D., & Kalcheim, C. (2002). Localized BMP4-noggin interactions generate the dynamic patterning of noggin expression in somites. *Developmental Biology*, **246**, 311–328.
- Selleck, M. A., & Stern, C. D. (1991). Fate mapping and cell lineage analysis of Hensen's node in the chick embryo. *Development*, **112**, 615–626.
- Stafford, D. A., Brunet, L. J., Khokha, M. K., Economides, A. N., & Harland, R. M. (2011). Cooperative activity of noggin and gremlin 1 in axial skeleton development. *Development*, **138**, 1005–1014.
- Stafford, D. A., Monica, S. D., & Harland, R. M. (2014). Follistatin interacts with noggin in the development of the axial skeleton. *Mechanisms of Development*, **131**, 78–85.

Stern, C. D., & Piatkowska, A. M. (2015). Multiple roles of timing in somite formation. *Seminars in Cell & Developmental Biology*, **42**, 134–139.

Streit, A., & Stern, C. D. (1999). Mesoderm patterning and somite formation during node regression: Differential effects of chordin and noggin. *Mechanisms of Development*, **85**, 85–96.

Teillet, M., Watanabe, Y., Jeffs, P., Duprez, D., Lapointe, F., & Le Douarin, N. M. (1998). Sonic hedgehog is required for survival of both myogenic and chondrogenic somitic lineages. *Development*, **125**, 2019–2030.

Tolkin, T., & Christiaen, L. (2016). Rewiring of an ancestral Tbx1/10-Ebf-Mrf network for pharyngeal muscle specification in distinct embryonic lineages. *Development*, **143**, 3852–3862.

Tonegawa, A., Funayama, N., Ueno, N., & Takahashi, Y. (1997). *Mesodermal subdivision along the mediolateral axis in chicken controlled by different concentrations of BMP-4*. *Development*, (Vol. **124**, pp. 1975–1984). Development.

Tonegawa, A., & Takahashi, Y. (1998). Somitogenesis controlled by noggin. *Developmental Biology*, **202**, 172–182.

Vasiliauskas, D., Hancock, S., & Stern, C. D. (1999). SWiP-1: Novel SOCS box containing WD-protein regulated by signalling centres and by Shh during development. *Mechanisms of Development*, **82**, 79–94.

Wijgerde, M., Karp, S., McMahon, J., & McMahon, A. P. (2005). Noggin antagonism of BMP4 signaling controls development of the axial skeleton in the mouse. *Developmental Biology*, **286**, 149–157.

Zee, T., Boller, S., Gyory, I., Makinistoglu, M. P., Tuckermann, J. P., Grosschedl, R., & Karsenty, G. (2013). The transcription factor early B-cell factor 1 regulates bone formation in an osteoblast-nonautonomous manner. *FEBS Letters*, **587**, 711–716.